Structural basis for sulfatide recognition by Disabled-2

Wei Song

Dissertation submitted to the faculty of the Virginia Polytechnic Institute and State University in partial fulfillment of the requirements for the degree of

Doctor of Philosophy
in
Biological Sciences

Daniel G. S. Capelluto, Chair
Carla V. Finkielstein
Chang Lu
William Huckle

December 10th, 2020
Blacksburg, VA

Keywords: Disabled-2; sulfatide; liposome; platelet activation; peptide-lipid interaction

Structural basis for sulfatide recognition by Disabled-2

Wei Song

Abstract

Disabled-2 (Dab2) is an adaptor protein that plays critical roles in various biological processes, including protein endocytosis, platelet activation and aggregation, tumor growth, and development. In platelets, Dab2 associates with membrane sulfatide at the platelet surface, modulating platelet inside-out and outside-in signaling pathways. A Dab2-derived peptide, named the sulfatide-binding peptide (SBP), is the minimal unit of Dab2 to exert its function as a negative regulator of platelet activation and aggregation. The work of this thesis refines the model of Dab2 SBP binding to sulfatide and provides structural and functional insights into the mechanism by which Dab2 SBP modulates platelet activation.

Using molecular docking, lipid-protein overlay assay, nuclear magnetic resonance, and surface plasma resonance tools, this work identifies the critical residues within two major regions responsible for sulfatide interaction. First, docking a sulfatide to Dab2 SBP, a hydrophilic region, primarily mediated by Arg42, is thought to be responsible for the association with the sulfatide headgroup. We observed that Arg 42 could directly interact with sulfatide by forming hydrogen bonds with the OS atoms in the sulfatide head group. Further lipid-protein overlay assay and surface plasma resonance experiments confirmed that both the positive charge and stereochemistry of the side chain of Dab2 SBP Arg42 are required for the sulfatide binding. Moreover, Arg42 is found to be critical in the inhibition of P-selectin expression on activated platelets. The residues nearby Arg42 (i.e., Glu33, Ty38, and Lys 44) also contribute to sulfatide interaction. Second, the second polybasic motif located at the C-terminal α-helix 2 is considered to interact with the acyl chain through hydrophobic interactions rather than direct binding to the charged sulfatide head group. Lysine residues in this region are suggested to exert a dual role in sulfatide association, that is, by favoring electrostatic interactions with the negatively-charged sulfatide and/or by employing their flexible hydrocarbon spacers for hydrophobic interactions with membrane lipids. Consistent with this suggestion, we found a hydrophobic patch in the wild type Dab2 SBP structure surrounded by Lys49, Lys51, and Lys53. Furthermore, the role of the second sulfatide binding

motif in sulfatide binding is confirmed by mutagenesis analysis and lipid-protein overlay assays, highlighting the ability of molecular docking to accurately predict critical residues responsible for sulfatide binding.

In summary, this work provides a detailed structural basis for Dab2 recognition by sulfatide through multiple biophysical methods. The corresponding biological implications in the inhibition of platelet activation are also evaluated by flow cytometry. By elucidating the underlying mechanisms of Dab2 mediating platelet activation through sulfatide binding, we provided structural and functional insights for designing a Dab2-derived peptide with altered sulfatide recognition features in platelets, which can be further employed in antiplatelet therapy.

Structural basis for sulfatide recognition by Disabled-2

Wei Song

General Audience Abstract

Platelets are blood cells that are fundamentally intended to help form clots to stop bleeding. They do so by being activated after getting signals from damaged blood vessels and reaching the injury site. Consequently, they form aggregates by attracting more platelets to clump on the clot. However, platelet activation induced by a tumor cell can, in turn, protect the tumor cell from immune system elimination and facilitates their growth and spread. This platelet-tumor complex formation suggests platelets as a therapeutic target for reducing tumor migration out of the bloodstream. Our study investigates the mechanism of a Disabled-2-derived peptide, named Dab2 SBP, which upon binding to a sulfatide lipid, can reduce the platelet activation extent, using molecular and cellular approaches. The results of this study may be instrumental in the generation of Dab2 SBP-derived peptides with altered sulfatide binding ability and selectivity, which may lead to a design of an antiplatelet drug that can limit the ability of tumor cells to invade other tissues.

Acknowledgement

I cannot believe I am finishing my Ph.D. study and writing this thesis here. I still remember my first day in America, excited but a bit disconcerted being thousands of miles away from my family and in a new culture. Four years have passed. Now here I am more confident and equipped for my future career and life. I appreciate all the people I have met during the past four years that make me who I am today.

First, I would like to express my deepest appreciation to my advisor, Dr. Daniel Capelluto, who relentlessly supported me throughout the graduate education and writing of this thesis. His patience, enthusiasm, motivation, and kindness have deeply inspired me. He has taught me the methodology to carry out the research and to present the work clearly to audiences in different fields. His guidance has shaped the way I think and see the problem. I am also grateful for his friendship and encouragement. He is not only the advisor of my research but also a mentor of life. I cannot count how many times he had taught me to stay positive when I was frustrated by some seeming-useless experimental data. From there, I have also learned how to find positive sites when life gets me down, even in the worst of times. I could not have imagined having a better advisor and mentor like him.

I would like to extend my sincere thanks to the rest of my committee members, Dr. Carla Finkielstein, Dr. William Huckle, and Dr. Chang Lu, for their insightful comments and suggestions on my research project. I am grateful to Dr. Finkelstein for her invaluable advice on improving the platelet isolation and flow cytometry setup, which enabled me to overcome the bottleneck that I was stuck on for over a year. I am grateful to Dr. Huckle for his constructive questions, which inspired me to deeply dive into my data when something seems not working. I am grateful to Dr. Lu for offering comments on my project and offering presentation suggestions that equipped me for the future career by practicing from each committee meeting. Special thanks go to Dr. Finkelstein. I appreciated that she cared for me and checked with me frequently when I was pregnant. She was so warm-hearted to take off my backpack when I was out of breath during my eight-month pregnancy after running out of the chilling wind to the lab.

I would also like to thank our collaborators, Dr. Anne Brown and Dr. Jeffrey Ellena, for their great contributions to the molecular docking and NMR studies, respectively. Their insights and suggestions made it much easier to proceed in the right direction. Without their contribution, I would not have completed my research and made it through my Ph.D. degree.

Going through my dissertation required more than academic support. I have many great people to thank for listening to and unwavering personal and professional support over the past four years and a half. I would like to thank my lab mates, Tuoxian Tang, Wen Xiong, and Tiffany Roach. I appreciate the invaluable experimental operations and tricks that Tuoxian and Wen taught me when I was pretty new to this lab. I appreciate all the helps Tuoxian offered whenever I was overwhelmed with my little one. I appreciate Tiffany for letting me go first whenever we have conflict schedules for the instrumental use. Besides a colleague, she is also a good friend. She is thoughtful to spot my tiredness and generously expresses her care and love to encourage me. I would also like to thank all undergraduates that I've met in the lab, especially Andrew Biscardi, Yejin Seo, Neha Reddy, Bridgit Spruill, Josephine Beyer, Robert Wallace and Evan Littleton. Thanks for introducing me to the many American cultures and making the workplace a whole lot of fun.

Special thanks go to Janet Rinehart, who volunteered to do the blood draw for us whenever I had a need. She never said no to me, even I asked for an early morning or when she was super busy with her work. I appreciate that she spared time for me no matter where she was working on the day. I am also thankful for her kindness of offering help to find blood donors even though I did not ask.

Special thanks also go to Natalie Brantly, a great mother of three boys. I met her when she was volunteering in our lab. Meeting Natalie changed my life. She radiates passion through everyone she met. I feel inspired by her energy and resilience every time we met up. Without her encouragement, I could not have an adorable boy by completing my Ph.D. degree.

Many thanks go to the support from ICTAS. Thanks for awarding me this fellowship. I am much lucky to be a member of predoctoral scholars. Thanks for providing us such an incredible platform to meet so many outstanding scholars from different fields.

At the end, I would like to express my deepest love to my parents and my husband, who support me, believe in me and love me. Thank you so much for everything!

Table of contents

Abbreviations

ADP	Adenosine 5′-diphosphate
AGD	Ala-Gly-Asp
AP-2	Adaptor protein-2
cAMP	Cyclic AMP
CD1a	Cluster of differentiation 1a
CTCs	Circulating tumor cells
Dab1	Disabled-1
Dab2	Disabled-2
dDab2	*Drosophila Disabled*
Doc-2	Differentially expressed in ovarian cancer
DPC	Dodecylphosphocholine
DPC	N-dodecylphosphocholine
DPF	Asp-Pro-Phe
DPPC	1,2-dipalmitoyl-sn-glycero-3-phosphocholine
DPPE	1,2-dipalmitoyl-sn-glycero-3-phosphoethanolamine
ECM	Extracellular matrix
EH	Eps15 homology
EMT	Epithelial-mesenchymal transitions
FCHO2	F-BAR FCH domain only-2
GM3	Glycosphingolipid monosialodihexosylganglioside
GPCR	G protein-coupled receptor
GPIb-IX-V	Glycoprotein Ib-IX-V-receptor
GPIIb/IIIa	Glycoprotein IIb/IIIa
GPVI	Glycoprotein VI
hDab2	human Dab2
LDL	Low-density lipoprotein
LDLR	Low-density lipoprotein receptor
MANF	Mesencephalic astrocyte-derived neurotrophic factor

MAPK	Mitogen-activated protein kinase
MVB	Multivesicular bodies
N-PTB	N terminal PTB domain
NPF	Asn-Pro-Phe
PKC	Protein kinase C
PRP	Platelet-rich plasma
PSGL-1	P-selectin glycoprotein ligand-1
PTB	Phosphotyrosine-binding
PtdIns(4,5)P_2	Phosphatidylinositol (4,5)-bisphosphate
RA	Retinoic acid
RGD	Arg-Gly-Asp
RGDS	Arg-Gly-Asp-Ser
SBMs	Sulfatide-binding motifs
SBP	Sulfatide-binding peptide
SPR	Surface plasmon resonance
TCIPA	Tumor cell-induced platelet aggregation
TGFβ	Transforming growth factor beta
TPA	12-O-tetradecanoylphorbol-13-acetate
TXA2	Thromboxane A2
UCB	Urothelial carcinoma of the bladder
vWF	von Willebrand factor

Chapter 1 Introduction

1. Platelet

1.1 Platelet production

Platelets are indispensable components in hemostasis. They also play critical roles in other fundamental biological processes, including innate immunity, wound healing, inflammation, and angiogenesis [1]. Human platelets are the second most numerous blood cells, with an average of 150-450 $\times 10^9$/L [2]. Each megakaryocyte in the bone marrow can produce over 5,000 platelets. Approximately two thirds of the platelets are released into the blood circulation and a third is stored in the spleen [3]. It takes ~5 days for megakaryocytes to produce and release platelets in humans [4]. Once released into the bloodstream, human platelets survive for 5-7 days [5] after of which are removed by macrophages in the spleen and liver.

1.2 Platelet structure

Platelets are anucleated cells with 2-5 μm in diameter and 0.5 μm in thickness [6]. Platelets are not true cells but are classified as circulating fragments of cells. Because they lack nucleus, they do not have nuclear DNA. However, they have mitochondria and mitochondrial DNA as well as structures that are crucial to stop bleeding. The platelet plasma membrane contains various surface receptors and lipid rafts, contributing to multiple signaling cascades and intracellular trafficking. Also, platelets contain a multitude of secretory granules, which serves pivotal functions for normal platelet function. Human platelets have two major kinds of organelles involved in secretion, α-granules and dense granules. The α-granule is the most predominate organelle, with 40-100 per platelet depending on the platelet size [6]. The membrane proteins of α-granules are expressed on the platelet plasma membrane during degranulation. Most of these proteins are also located on the resting platelet surface, such as integrins (e.g., αIIbβ3) and immunoglobulin family receptors (e.g., glycoprotein VI (GPVI)), while some of the membrane proteins in α-granules are not present on the resting platelet surface, such as P-selectin [3] and CD109 [7]. Instead, they are expressed on the platelet surface after activation. α-granules also contain soluble proteins that are released to extracellular space following activation. The proteins in α-granules are diverse concerning function, including adhesive proteins (e.g., fibrinogen, P-selectin, and αIIbβ3 integrin), coagulant factors and co-factors (e.g., factors V, XI, and XIII), and anti-coagulants (e.g., Disabled-2). The

less prevalent platelet dense granules are composed of large amounts of active molecules that enhance platelet activation, including Ca^{2+}, adenosine 5′-diphosphate (ADP), serotonin, and histamine [8].

1.3 Platelet activation and aggregation

The principal function of platelets is to form clots and stop bleeding at the site of damaged endothelium. They do so by being activated after getting signals from damaged blood vessels and reaching the injury site. The blood vessel walls are lined by a one-cell thick layer of endothelial cells. Vascular injury leads to collagen and tissue factor exposed in the subendothelial extracellular matrix (ECM) to the flowing blood. Within seconds, initial platelets adhere to the damaged blood vessel *via* binding of the GPIbα subunit of surface glycoprotein Ib-IX-V-receptor (GPIb-IX-V) to the von Willebrand factor (vWF) immobilized on subendothelial-exposed collagen fiber. Both GPIbα and VWF undergo conformational changes to increase their binding affinity, allowing platelet adhesion under shear stress, particularly at high flow shear rates [9]. Subsequently, transiently rolling platelets become able to tightly adhere to collagen *via* the GPVI, promoting a more firm adhesion [10] and further platelet activation. Binding of GPVI to collagen results in an increased cytosolic calcium level and the transition of platelet αIIbβ3 integrins from a close state for extracellular ligands to an active state, which favors extracellular ligands binding and triggers platelet adhesion and aggregation. This process is referred to as inside-out signaling [11]. Many granule cargoes are also released, potentiating platelet activation and stabilize platelet aggregates at the site of injury. These granules cargoes include vWF, P-selectin, and fibrinogen from α-granules, and ADP, calcium, and serotonin from dense granules. Furthermore, increased calcium levels triggers rapid cytoskeletal reorganization, inducing the change of platelet shape from the normal concave discs to a compact sphere with pseudopodial extension, facilitating platelet adhesion and spreading on the adhesive surface [2]. Finally, platelet αIIbβ3 integrin interacts with vWF, endothelial vitronectin, and soluble fibrinogen, which bridges platelets and endothelial cells as well as adjacent platelets.

During platelet activation, many receptors are also activated other than αIIbβ3 integrin receptors. Ligand binding to receptors not only regulates platelet adhesion and aggregation but also stimulates intracellular signal events, which leads to stable platelet adhesion, spreading, granule

secretion, and irreversible aggregation in the early phase and clot retraction in the later stage. This process is known as platelet outside-in signaling. Therefore, platelet activation requires the cooperation of various receptors containing various signals, with each contributing for the formation of a platelet plug.

1.4 Platelet activation by ADP

Platelets activation can be induced by soluble agonists released at the site of vascular injury or from activated platelets. One of the essential activators, ADP, is present in the dense granule and released after activation or from the site of injury. ADP, a weak agonist of platelet activation, induces only reversible cascades when compared to strong agonist like thrombin. However, all the other platelet agonists are, more or less, dependent on ADP release to achieve maximal platelet aggregation, and this dependence is in a dose-dependent manner and varies with the agonist [12]. Consequently, ADP is also called a secondary agonist that strengthens most of the platelet responses, assisting in the recruitment of additional platelets and stabilizing the thrombus [13]. Interestingly, ADP activation is thought to be required for sulfatides to exhibit their activating functions on platelets as the addition of sulfatides to unstimulated platelets did not show any activation effects [14].

In vitro studies showed that when ADP was added to platelets, a signaling cascade occurred, including thromboxane A2 (TXA2) formation, protein phosphorylation, a rise in cytosolic calcium, cell shape change, granule secretion and aggregation [12]. Like other soluble agonists, ADP induces platelet activation *via* interaction with the G protein-coupled receptor (GPCR) on the platelet membrane. ADP functions through two purinergic GPCRs, P2Y1 (~150 copies per platelet) and P2Y12 (~600 copies per platelet) [12]. ADP binding to P2Y1 leads to a transient increasement of intracellular Ca^{2+}, inducing platelet shape change and fast reversible platelet aggregation. Platelet aggregation is strengthened by ADP binding to P2Y12, which stimulates adenylyl cyclase inhibition, reduced cyclic AMP (cAMP) levels and amplified secretion and aggregation caused by other agonists [15]. An optimal platelet aggregation response to ADP *in vitro* requires the coactivation of P2Y1 and P2Y12, as platelet function is compromised if any of them or their coupled G proteins are inhibited or deleted [16–18]. Most notably, the effects resulting from the deletion of P2Y1 and P2Y12 in mice [19] are in line with those predicted by pharmacological investigations in human platelets [16].

1.5 Interplay between platelets and tumor cells

Metastasis describes the process of cancer cells spreading from the originated site to surrounding tissues and to distant sites. Remarkably, over 90% of cancer deaths is caused by metastasis [20]. Within the bloodstream, circulating tumor cells (CTCs) can directly stimulate platelet through various mechanisms. The activated platelets adhere to tumor cells forming heteroaggregates, which shield CTCs from the lysis of the immune system and the shear stress of blood flow, facilitating tumor cell survival [21] and establishing secondary lesions [22]. The survived tumor cells further trigger platelet activation. Tumor cells secrete TXA2 and ADP, which provide a positive feedback loop that amplifies platelet activation and causes tumor cell-induced platelet aggregation (TCIPA), facilitating CTCs survival within the circulation. ADP release has been observed in the aggregation complex of platelet and colon cancer cells. The inhibition of ADP activity has been associated with reduced aggregation of platelet and tumor cells, indicating ADP serving as a promotor for tumor cell survival [23]. Moreover, platelet activation leads to the granules degranulation and secretion, resulting in the release of myriad of growth factors, cytokines, angiogenic protein and mitogenic proteins that reciprocally act on tumor cells to support tumor cell establishment at distant sites. Therefore, the interplay between platelets and tumor cells exists, with tumor cells triggering platelet activation and activated platelets promoting tumor cell survival and growth [24]. The link between platelets and tumor invasion and migration offers therapeutic opportunities for manipulation in platelet-mediated extravasation support.

2. Disabled-2 (Dab2)

Disabled 2 (Dab2) has been implicated in many signaling processes, particularly in endocytosis and platelet function [25]. During clathrin-mediated endocytosis, Dab2 is an adaptor protein that recruits protein cargoes and lipids to the cell membrane where endocytosis occurs. In platelets, cytosolic and extracellular Dab2 modulate platelet function through the association with αIIbβ3 integrin in different regions. Extracellular Dab2 also interacts with the platelet surface sulfatides to control the extent of platelet activation and aggregation. Notably, Dab2 also exerts a multifaced role in tumorigenesis and metastasis.

2.1 Dab2 discoveries and isoforms

Dab2, a mammalian ortholog of the *Drosophila Disabled* (dDab2) gene, is 30% homologous to dDab2 and shows 45% identity and 60% sequence homology to Disabled-1 (Dab 1), the other

mammalian ortholog [26]. In comparison, Dab2 is distributed in various tissues, such as brain, kidney and intestine, whereas Dab1 specifically functions in the brain [27].

Historically, Dab2 was identified as a phosphoprotein with a size of 96 kDa in the murine BAC1.2F5 macrophage cell line, and it undergone a rapid phosphorylation due to the stimulation caused by colony-stimulating factor 1 [28]. Accordingly, Dab2 is termed as p96. Human Dab2 (hDab2) is also designated as DOC-2 (differentially expressed in ovarian cancer) due to its gene was characterized as the tumor suppressor gene of ovary cancer [29]. The *Dab2* gene is present at chromosome 5p13, and it encodes a protein of approximately 96 kDa with 770 amino acids. The *Dab2* gene is expressed as two spliced isoforms, which are designated as p96 and p67 in mice and humans, and p82 and p59 in rats[30]. Thus, p96 is also referred to as p82, and p67 is also known as p59. p96 contains 15 exons, while p67 lacks the ninth exon corresponding to 230-447 amino acids in p96. Correspondingly, several binding sites for endocytic proteins are lost in p67. Unlike p96, p67 is less efficient in endocytosis as it cannot bind to clathrin and the adaptor protein-2 (AP-2) [31].

2.2 Regulation of Dab2 expression

The expression level of Dab2 has been reported to be regulated by various factors. Both p96 and p67 isoforms can be strongly upregulated by retinoic acid (RA) during mouse embryonic development [32]. Dab2 expression can be induced by GATA factors during the RA-induced F9 embryonic carcinoma cell differentiation [32]. Dab2 has also found to be inhibited by oncogenic Ras [33], supported by the finding that Dab2 was significantly downregulated in hyperplastic urothelium in Ras transgenic mice [34]. A reciprocal regulation between Dab2 induction and mitogen-activated protein kinase (MAPK) activity was also suggested in the megakaryocytic differentiation of K562 cells [35].

2.3 Dab2 is a cargo-selective endocytic clathrin adaptor

Clathrin-mediated endocytosis plays a crucial role in vesicular trafficking, through the transportation of numerous cargo molecules from plasma membrane. It is a predominant mechanism of eukaryotic cells internalizing extracellular molecules, reorganizing receptors, and regulating intercellular signaling. The endocytic adaptors associate with clathrin, phosphatidylinositol (4,5)-bisphosphate (PtdIns(4,5)P_2), and the cytosolic tails of different transmembrane cargoes containing internalization signals, thus recruiting cargoes to the region of

the plasma membrane where the vesicles form. Dab2 is one such adaptor implicated in clathrin-mediated endocytosis and cargo trafficking, by favoring multiple interactions through its domains and sequence motifs (Figure 1).

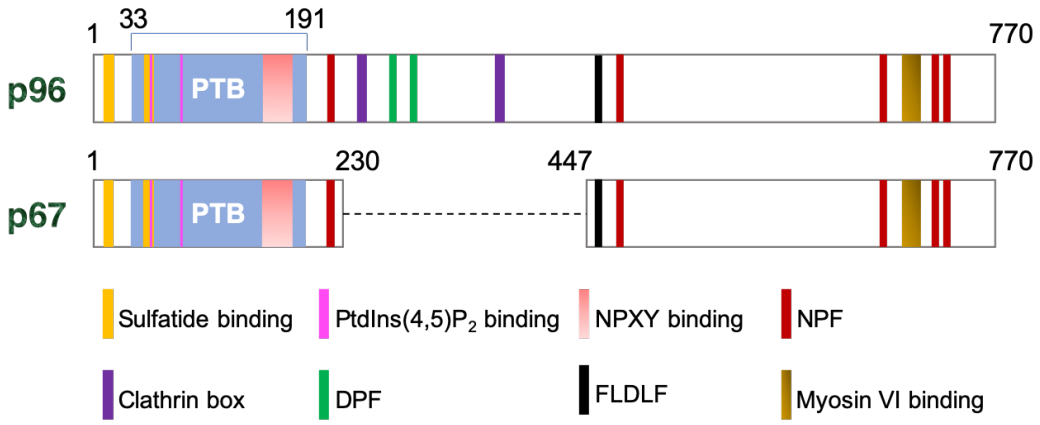

Figure 1. Schematic representation of Disabled-2 (Dab2) isoforms with their conserved domains and motifs. Human Dab2 is represented by two isoforms, p96 (top) and p67 (bottom). Dab2 ligand-binding regions are color coded.

Sequence homology shows that mammalian Dab2 structure and domains are closely related to many endocytic adaptor proteins, such as Dab1, Numbl, Numb, and Arh [36]. Studies in Dab2 knockout mice suggested that Numb and Arh can provide compensatory expression[37] and partial functional redundancy during embryonic development [38]. The highest sequence homology among Dab2, Dab1, Numb and Arh is found at the N-terminus, where the phosphotyrosine-binding (PTB) domain is found.

The Dab2 two isoforms, p96 and p67, also share the evolutionarily conserved N-terminal PTB domain (residues 33-197), which exerts significant functions in protein-protein and protein-lipid interactions involved in endocytosis. The original characterization of PTB domain indicates that it is a domain that binds to the NPXY motif containing tyrosine phosphorylation [39]. Interestingly, the PTB domain has also been found to interact with non-phosphorylated NPXY motifs and non-tyrosine motifs [40]. For example, through the PTB domain, Dab2 recognizes non-phosphorylated NPXY motifs contained in many cargo transmembrane proteins, such as integrins, megalin, low-density lipoprotein (LDL) receptors (LDLR), amyloid precursor protein, and apolipoprotein E receptor [25,41]. The PTB domain can also bind phosphoinositides, preferentially PtdIns(4,5)P_2 [42], a critical phosphoinositide for endocytosis [43]. Moreover, this interaction coincides with the

association of Dab2 and the NPXY motif in cargo proteins, facilitating Dab2 membrane targeting [41]. Indeed, the interaction between adaptor proteins (e.g., Dab2) and PtdIns(4,5)P_2 head groups has been proposed to play a part in membrane curvature formation and lipid bilayer destabilization to trigger membrane deformation [44]. A supported finding suggested that Dab2 can convey LDL receptor into clathrin-coated pits through interaction with PtdIns(4,5)P_2, independently of the presence of the clathrin adaptor protein 2 (AP-2) or Arh adaptor protein [42].

The middle region of Dab2 is alternatively spliced, being absent in the p67 variant (Figure 1). This p96-exclusive middle region consists of two clathrin boxes, two DPF (Asp-Pro-Phe) motifs and one NPF (Asn-Pro-Phe) motif. Dab2 binds to clathrin directly on its heavy chain and interacts with pre-assembled clathrin cages, allowing soluble trimeric clathrin to effectively assemble closed clathrin cages [45]. AP-2 is historically considered as a master regulator of the clathrin-mediated endocytosis, which regulates receptors, clathrin, and other essential factors at the cell membrane. The DPF motifs in Dab2 can directly interact with the α-adaptin subunit of AP-2 [44] and contribute to the assembly of the clathrin-coated pits. The DPF motifs also interact with the F-BAR FCH domain only-2 (FCHO2), a protein that regulates the number and size of clathrin structures. Like Dab2 binding to AP-2 [46], one DPF motif is considered sufficient to recognize FCHO2 [47]. It is worth noting that AP-2 can compensate for the loss of the binding of Dab2 to FCHO2, whereas Dab2-FCHO2 interaction is indispensable for endocytosis of Dab2-targeted cargo in the case of AP-2 absence [47]. It has been proposed that competition likely exists between FCHO2 and AP-2 for Dab2 DPF motif binding to regulate molecule organization of a clathrin-coated pit. Also, the sequential association of FCHO2 and AP-2 to the Dab2 DPF motif is suggested to make a contribution to the development of a clathrin-coated pit [47].

The middle and C-terminal region of both p96 and p67 contain four additional NPF motifs. A total of five NPF motifs regulate the recognition of Dab2 to Eps15 homology (EH) domain proteins, Eps15 and intersectin, thus, driving integrin β1 (the Dab2 cargo) internalization and facilitating clathrin assembly [48]. Although all five NPF motifs in p96 show binding to Eps15 and intersectin, the three located at the C-terminal show much stronger interaction than the two in the central region [48]. The C-terminal of the protein also contains another AP-2-binding sequence, FLDLF [45], a binding site for myosin VI [49], and sites for SH3-domain proteins [50]. Myosin is also known to interact with PtdIns(4,5)P_2 with a high affinity (K_D=0.3 μM) and in a calcium-dependent manner.

Therefore, Dab2 and PtdIns(4,5)P_2 binding coordinately mediate the myosin VI recruitment to clathrin-coated structure at the plasma membrane [51]. By binding to myosin VI, Dab2 mediates the simultaneous attachment of transmembrane cargo proteins containing NPXY motif to the myosin VI, engaging endocytosis and unidirectional trafficking.

2.4 Dab2 is a two-face regulator in tumorigenesis and metastasis

Over the past two decades, the studies on the role of Dab2 in tumorigenesis and development have attracted increasing attention. The experiments leading to the discovery of Dab2 (DOC-2) were based on its consistent absence in multiple human ovarian cancer cell lines [29]. A few years after, it was reported that the Dab2 expression could be observed in ovarian and breast epithelial cells with normal biological immortality, but not in 90% of tumor cell lines derived from breast and ovarian epithelial tumors [52]. Indeed, Dab2 downregulation was also detected in 80% of mammary tumors in mouse mammary carcinogenesis model [53]. To date, accumulated evidence has demonstrated that Dab2 is decreased or lost in a wide variety of cancers other than ovarian and breast cancer, including lung cancer [54], colorectal cancers [55], nasopharyngeal cancers [56], pancreatic carcinomas [57], bladder carcinomas [34], gastric cancers, meningiomas [58] and esophageal squamous tumors [59]. Consequently, these findings indicate the role of Dab2 as a tumor suppressor. Furthermore, lost Dab2 expression is found strongly correlated to the transition of ovarian surface epithelial cells to pre-malignant phenotypes [59,60]. Likewise, loss of Dab2 expression is observed in the early pre-neoplastic stages of esophageal squamous tumorigenesis [59]. Nevertheless, the underlying mechanism of how Dab2 executes these effects is not fully understood.

The epithelial-mesenchymal transitions (EMT) is a highly dynamic process by which epithelial cells loose cellular polarity and cell-cell adhesion, obtain improvements in migratory and invasive characteristics and convert into mesenchymal phenotype [61]. EMT is becoming a potential target for cancer therapy due to its contribution to the tumor progression with metastatic expansion and the generation of tumor cells bearing stem cell characteristics, which play a significant role in cancer treatment resistance. Many studies suggest that altered Dab2 levels directly or indirectly lead to EMT. Dab2 negatively regulates EMT through different signaling pathways, including TGFβ (transforming growth factor beta) and Wnt signaling pathways, which are associated with EMT and the development of many tumor types [62–65]. Reduced expression of Dab2 induces the activation of the Ras/MAPK signaling cascade, causing an increased TGFβ and a stable EMT in

breast tumor cells [66]. Similarly, the downregulation of Dab2 was found to stimulate the induction of EMT in pancreatic cancer cells through activation of TGFβ and MAPK signaling pathways [57]. In addition, decreased expression of Dab2 in lung cancer causes the aberrant activation of the Wnt pathway and promotes the proliferation and invasiveness of tumor cells [67]. Collectively, these findings indicate that Dab2 acts as a negative regulator of tumor cell growth and proliferation.

However, accumulated evidences show that Dab2 is also required to promote cell development phenotype in normal and pathological cells. In normal murine mammary gland cells, Dab2 is up-regulated and accumulated on the membrane by binding to β1 integrin during TGFβ-induced EMT, while downregulated Dab2 inhibits TGFβ-mediated EMT and trigger apoptosis [68]. EMT occurs in both physiological and pathological cellular states. It is well established that signaling pathways modulating EMT share commonalities for early embryonic development and tumor progression [68]. The pro-apoptotic function of Dab2 in normal cells suggests a similar molecular mechanism occurring in tumor cells. In 2015, studies in human prostate cancer cells showed that Dab2 knockdown inhibits the migratory, invasive abilities and tumorigenicity, whereas Dab2 overexpression promotes the cell migration and invasion in PC3 cell lines [66]. More recently, increased expression of Dab2 was found in human urothelial carcinoma of the bladder (UCB), which correlated with the enhancement of EMT, tumor proliferation, migration as well as invasion. In contrast, the inhibition of Dab2 is able to result in tumor shrinkage and invasion suppression, which is suggested as a potential therapy to improve the prognosis of human UCB [69].

Several variables could be argued for the paradox among the above studies. First, the tissue- and region-specific differential expression pattern of Dab2 may readily explain the dual role of Dab2 in tumor progression. At the protein level, Dab2 is found expressed in many mouse tissues, including brain, heart, skeletal muscle, liver, lung, and highly abundant in brain [70], and kidney [52]. While in human tissues, Dab2 is also widely expressed, including brain [70], prostate, spleen, small intestine, testis, thymus, and particularly high in ovary [52] and breast tissues [27]. Despite some contradictory results, it is commonly accepted that the expression of Dab2 is frequently observed in ovary and breast cancers. Multiple evidences are obtained from studies using either various human cell lines *in vitro* or mouse models and patients' ovarian cancer specimens. The primary debate on whether Dab2 is a tumor suppressor or a tumor promoter lies in the studies in other cancer types, such as prostate and bladder cancers.

Second, Dab2 has two major spliced isoforms in human, p96 and p67. The Dab2 expression has been shown predominantly by immunohistochemistry staining and western blot, while not all reports in the field clearly stated which Dab2 isoform was targeted. The alternative splicing of Dab2 happens in a tissue-specific manner with a high expression of p67 in kidney and p96 in brain [70]. Even within the same tissue, p96 and p67 display a distinct distribution. For example, intestine studies revealed that p67 is specifically found in the apical membrane of the suckling ileum, whereas p96 is found in ileum, jejunum, enterocytes, and crypts with varying expression levels [72]. Additionally, studies on lung cancer [67] and breast cancer [71] both suggest that p96 and p67 exhibit different functions in the process of oncogenesis.

Lastly, the progression of the cancer stages may affect the evaluation of Dab2 levels. Indeed, the levels of Dab2 show distinct patterns in the development of different tissues. For example, Dab2 at both mRNA and protein levels increase with kidney development, whereas they decrease along with intestine maturation [72]. It is reasonable to speculate that Dab2 expression level may present a similar pattern in the development of cancer cells. Evidenced results from Itami *et al*. reveal that Dab2 expression increased dramatically along with UCB progression [69]. Although Dab2 is usually lost in meningioma cell lines, its variable expression level also depends on the grade of malignancy [58]. In addition, Dab2 exerts dual roles in ovarian cancer proliferation and progression regulated by miRNAs. In the initial stages of tumorigenesis, the tumor cell migration and proliferation is promoted due to a reduced expression of Dab2 mediated by microRNA (miRNA)-187. In contrast, in the later phases of tumor development, continued Dab2 inhibition also inhibits Dab2-dependent EMT [73]. Dab2 may be a putative tumor suppressor, but it also modulates the tumorigenesis by promoting EMT-mediated metastasis in late stages of cancer progression [68,74]. It must be noted that Dab2 is necessary but not sufficient for inducing EMT as upregulation of Dab2 alone does not cause any morphological changes related to EMT [74], indicating the presence and significance of crosstalk between Dab2 and other signaling molecules involved in the EMT process. In the transition into mesenchymal cells, epithelial cells apparently gain abilities to be resistant to apoptosis. In order to protect cells from apoptosis, Dab2 would promote invasiveness and tumor development. Epithelial cells originally benefit from the absence of Dab2 and gain genetic alterations, which enables the resistance to apoptosis. Alternatively, these benefited epithelial cells

may become less adhesive and more invasive, facilitating the metastasis formation during the late phase of tumorigenesis [68]. Over the decades, there are accumulated reports about the altered Dab2 expression in different solid tumors; the role of Dab2 in CTCs are barely reported. The major limitation may lie in the poor isolation of CTCs due to their availability in limited numbers, which takes endeavor to develop techniques with the high efficacy of CTCs isolation and enumeration [61].

2.5 Dab2 is a negative regulator of platelet activation and aggregation

2.5.1 Expression of Dab2 in megakaryocytes and platelets

Dab2 is first expressed during megakaryocytic differentiation, concomitantly with the integrin β3 subunit expression [75]. In platelets, Dab2 is highly expressed with a predominant distribution in the α-granules and the cytosol but it can also be found in early endosomes. The α-granules are enigmatic because they have both proteins derived from the megakaryocyte and proteins taken up by endocytosis [76]. However, the trafficking pathway of platelet α-granules is still unclear. The biogenesis of α-granules starts in megakaryocytes but continues in platelets [7]. The α-granules are suggested to generate from multivesicular bodies (MVB) and late endosomes in megakaryocytes [76]. Similarly, the dense granules are also produced from MVB/late endosome [77]. Recently, recycling endosomes are unveiled to be a key intermediate compartment between type I MVB and type II MVB. It is also known that soluble proteins have to be incorporated in vesicles generated from the *trans*-Golgi network to become cargo of mature α-granules [7]. Therefore, in megakaryocytes, the cytosolic Dab2 obtained from the endocytosis may be transported into early endosome or recycling endosomes, from where Dab2 moves towards type II MVB that matures to α-granules.

Dab2 is differentially expressed in platelets among different organisms. Murine platelets contain less amount of Dab2 compared with rats and human platelets. However, the expressions of Dab2 are all up-regulated during the differentiation of human leukemic K562 cells [35], human CD34+ hematopoietic pluripotent stem cells and murine embryonic stem cells [75]. The two splices isoforms, p96 and p67, also show different expression patterns in human, rat and murine platelets. Human and murine platelets only express p96 and p67, respectively, while both p96 and p67 can be detected in rat platelets [78].

2.5.2 Dab2 mediates platelet inside-out and outside-in signaling through integrin binding

The integrin αIIbβ3 is the most abundant integrin in platelets, playing critical roles in many aspects of platelet functions. It is also known as the glycoprotein GPIIb/IIIa (CD41/CD61) complex. Quantitative studies found that 50,000–100,000 copies of αIIbβ3 are present at the surface of resting platelets [79], and more αIIbβ3 molecules from the α-granule surfaces are fused to the plasma membrane after platelet activation, especially stimulated by soluble agonists, such as thrombin and ADP [80]. The integrin αIIbβ3 is typically in a close state with a low-affinity in circulating platelets, but switches to an activated state with high affinity for the ligands state on platelet activation. This process is known as inside-out signaling. Activated αIIbβ3 integrin binds to multiple Arg-Gly-Asp (RGD) motif-containing adhesive proteins, including vWF, fibrinogen, fibrin, fibronectin, and thus mediates platelet adhesion, platelet aggregation, and thrombus formation. Of these ligands, fibrinogen is the major ligand, which, together with vWF, mediates platelet aggregation in soluble form and adhesive spreading in solid phase [81]. Binding of fibrinogen to activated αIIbβ3 integrin also triggers the outside-in signaling of αIIbβ3. This signaling induces a intracellular signaling cascade, which mediates irrevocable platelet adhesion, spreading, and clot retraction as well as irrevocable platelet aggregation and shape change, and thus subsequent thrombus growth [41].

Dab2 exerts its dual role in fibrinogen-integrin binding by functioning in both the inside-out and outside-in integrin signaling pathways (Figure 2), which can be reflected by its subcellular distribution. The cytosolic Dab2 is thought as a negative regulator of the inside-out signaling, where cytosolic Dab2 is phosphorylated by protein kinase C (PKC) at Ser24. This phosphorylation promotes Dab2 membrane translocation [75], leading to Dab2 binding to the cytoplasmic tail of integrin β3 subunit and subsequent inhibition of integrin activity. By doing so, Dab2 blocks the inside-out integrin signaling and the following fibrinogen-mediated platelet adhesion. However, the fate of phosphorylated Dab2 after membrane recruitment is not clear. It is important to notice that Dab2, in the absence of Ser24 phosphorylation, is required in integrin-mediated cellular uptake of fibrinogen [82]. Dab2 may mediate fibrinogen internalization through its PTB domain as PTB binds to the NPXY motif in the integrin β3 subunit [83]. Interestingly, Ser723 phosphorylation in Dab2 is found in thrombin-mediated inside-out signaling and platelet activation [84], while it is unknown whether Ser723 phosphorylation coincides with Ser24 phosphorylation and whether Ser723 phosphorylation also plays a role in membrane translocation of Dab2. On the cell membrane, the integrin-bound Dab2 also interacts with PtdIns(4,5)P_2 (Figure 2), which is proposed

to facilitate the recruitment of cytosolic Dab2 to the platelet membrane. Supportive observations indicate that PtdIns(4,5)P_2 binding facilitates Dab2 membrane recruitment [41]. Also, PtdIns(4,5)P_2 is required for Ca^{2+}-induced secretion of Dab2-containing α-granules [85], and its expression is increased in the intracellular membrane of activated platelets [86]. Likewise, Dab1, the other mammalian homolog of Dab2 protein, has also been suggested as a negative regulator of platelet activation and adhesion [41].

Dab2 can also be found at the α-granules of human megakaryocyte and platelets under resting conditions. After platelet is stimulated by soluble agonists, such as collagen, thrombin, ADP, and 12-O-tetradecanoylphorbol-13-acetate (TPA), α-granules secrete Dab2 in a PKC-dependent manner [14]. Dab2 is exposed at the platelet surface following fusion of the α-granules with the extracellular membrane, where Dab2 plays a role in the integrin outside-in signaling and inhibits platelet aggregation. To do so, Dab2 interacts with both αIIbβ3 integrin and sulfatides. The balance between these two interactions is believed to be necessary to regulate the platelet aggregation, clotting retraction, and the interactions of platelets with fibrinogen upon stimulation by soluble agonists [25,87]. Dab2 associates with the external region of the integrin αIIb subunit *via* the RGD motif (residues 64-66 in hDab2) within its PTB domain. A mutation in the Dab2 RGD motif abolishes the integrin binding as observed from fibrinogen binding assay and flow cytometry [75]. Although αIIbβ3 integrin interacts with both the RGD and AGD (Ala-Gly-Asp) motifs in fibrinogen [88], the Dab2 RGD motif is thought as competent to occupy the RGD binding region within αIIbβ3 integrin, thus preventing fibrinogen binding to integrin, which builds the basis of platelet aggregation inhibition by Dab2. In fact, Dab2 binding to integrin has been suggested as required and sufficient to prevent platelet adhesion and aggregation through sequestering fibrinogen interaction with αIIbβ3 integrin [87]. Further molecular analysis on the binding affinity of integrin αIIbβ3 to Dab2 and fibrinogen should help understand the Dab2 functions in inhibiting fibrinogen-integrin mediated platelet aggregation.

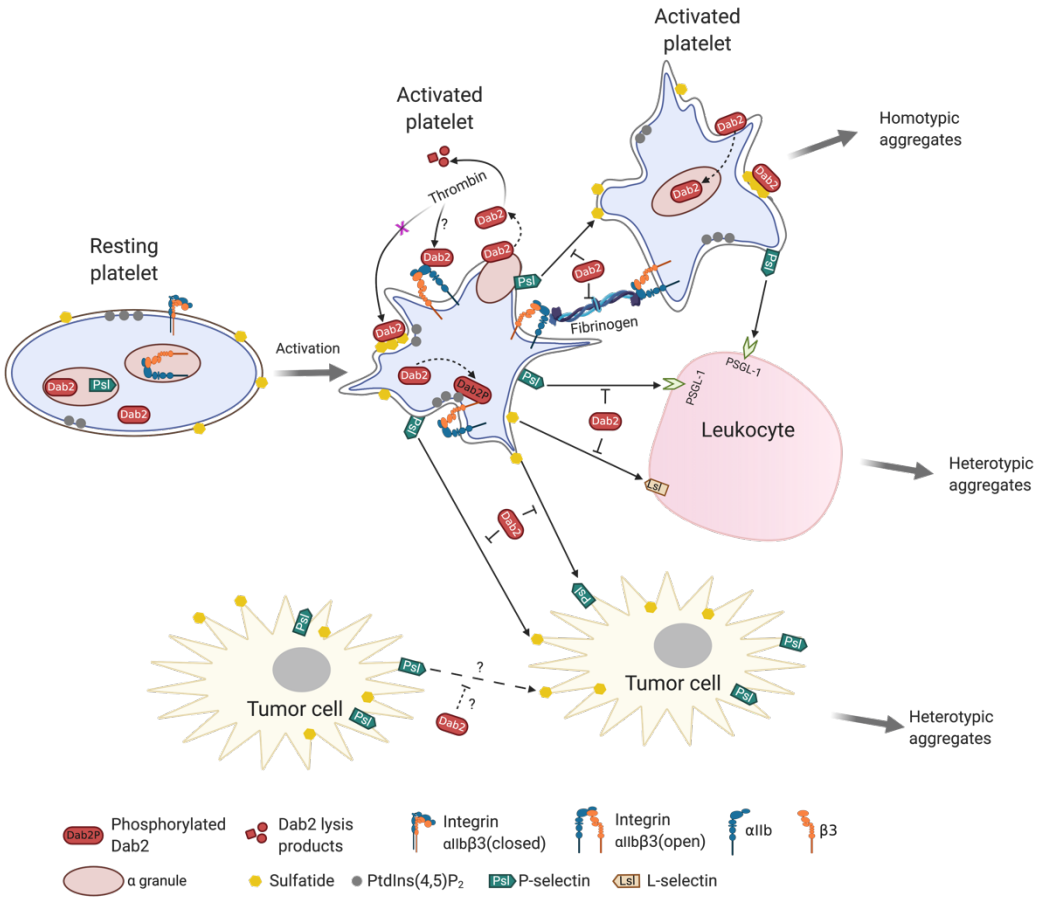

Figure 2. The model of Dab2 and sulfatide-mediated modulation of platelet homotypic and heterotypic interactions. In resting platelets, Dab2 is present in both α-granules and cytosol. Following activation, cytosolic Dab2 is phosphorylated by PKC and translocated to the inner leaflet of the plasma membrane, where it binds to the cytosolic tail of integrin β3 subunit, inhibiting the integrin receptor. Dab2 stored in the α-granules is secreted and released to the extracellular membrane of platelets, where it is distributed into two distinct pools. One pool of Dab2 binds to integrin αIIb subunit, blocking fibrinogen binding to the integrin, thus prevents clot formation by modulating platelet aggregation. The other pool of Dab2 binds to cell surface sulfatides. Extracellular Dab2 is a substrate of thrombin, while sulfatide association can protect Dab2 from thrombin cleavage. Dab2 is transiently present on the cell surface and can be internalized back to α-granules. Platelet surface sulfatides bind to both P-selectin and L-selectin, mediating platelet-platelet and platelet-leukocyte interactions, respectively. Platelet-leukocyte interactions can also occur through the association of P-selectin with PSGL-1. Dab2 negatively modules platelet homotypic interaction and heterotypic interaction. Certain tumor cells also express sulfatide and P-selectin on the cell surface, thus can interact with platelets through sulfatide-P-selectin binding, while it is unknown whether the association of sulfatide with P-selectin also occurs between two tumor cells.

2.5.3 Dab2 mediates outside-in signaling through sulfatide binding

Sulfatides (SM4, 3-O-sulfogalactosylceramide, or sulfated galactocerebroside) are sulfated glycosphingolipids localized mainly in the plasma membrane and membranes of the Golgi apparatus [89] and lysosomes [90]. At the plasma membrane, sulfatide is enriched at the outer leaflet and be part of lipid rafts [91]. It is well established that sulfatide exerts many critical biological functions, such as signal transduction, protein trafficking, cell adhesion, and aggregation [92]. In blood circulation, sulfatide can be found at the surface of erythrocytes, platelets [93], leukocytes, and neutrophils [94]. In platelets, the expression of sulfatide is increased upon activation [95]. In addition to Dab2, sulfatide binds to adhesion proteins, including vWF, laminin [96], thrombospondin [97], L-selectin [98], β2-glycoprotein I [99], and P-selectin [100] indicating a critical role of sulfatide in hemostasis. P-selectin expressed on the platelet surface determines the stability and size of the platelet aggregates [95]. Moreover, sulfatide interaction with P-selectin further promotes platelet activation and stabilizes platelet aggregates and platelet-leukocyte aggregates [101], triggering a positive feedback loop that enhances the platelet activation and stable platelet and platelet-leukocyte aggregations.

Extracellular Dab2 also binds sulfatides at the cell surface after platelet activation (Figure 2). Dab2 association with sulfatide involves residues Lys25, Lys49, Lys51, and Lys53 within the two conserved polybasic sulfatide-binding motifs (residues 24-29 and 49-54, respectively). These two motifs are characterized as XBBXBX (B, basic residue; X, any residue) and BXBXBX motifs, and they are reported to mediate sulfatide association with other adhesive proteins, such as laminins, thrombospondins, and selectins [102]. The first polybasic motif is found to be capable of inducing enlarged Dab2-clathrin assemblies and facilitating integrin-mediated cell spreading [103]. Lys53, located at the end of the second putative sulfatide binding motif, is one of the two residues responsible for recognizing PtdIns(4,5)P_2, while the other is Lys90. Therefore, the binding sites of Dab2 to sulfatides partially overlap with those involved in PtdIns(4,5)P_2 binding. However, competition binding is unlikely to occur between these two lipids as sulfatide and PtdIns(4,5)P_2 are predominately located at the outer [104] and inner leaflet [105] of the platelet membrane, respectively. Remarkably, both lipids play a role in enhancing protein stability against temperature-induced unfolding [106]. However, solution NMR spectroscopy studies revealed that the two lipids binding takes place through distinct binding mechanisms. Specifically, sulfatides association induces

conformational changes of Dab2 and facilitates Dab2 membrane penetration, whereas only minor local structural changes of Dab2 is detected upon PtdIns(4,5)P_2 binding, which primarily occurs through electrostatic interactions [106].

The PTB domain of Dab2 is a substrate of thrombin [41]. A putative thrombin cleavage site (Lys-30-Gly31) is found between the two polybasic motifs (residues 44-45 in hDab2) and confirmed by thrombin-limited proteolysis assay [87]. Unlike integrin-bound Dab2, which is susceptible to thrombin cleavage [14], sulfatide-bound Dab2 at the platelet surface protects Dab2 from thrombin proteolysis [87]. Therefore, one pool of Dab2 can be unimpaired at the platelet surface, facilitate its role in mediating platelet aggregation. On the other hand, PtdIns(4,5)P_2 binding cannot protect the PTB domain from thrombin cleavage [87], highlighting the role of sulfatide in Dab2 stabilization during thrombin-mediated activation. In addition, sulfatide binding also modulates the redistribution of Dab2 on the cell membrane as a mutant with mutations in the two sulfatide binding motifs exhibited a decreased presence at the plasma membrane of activated platelets [87]. However, the presence of Dab2 at the platelet surface is transient due to a rapid protein internalization back to α-granules in an actin-dependent, but clathrin-independent, manner [87].

Furthermore, sulfatide binding by Dab2 also competes with sulfatide interactions with lectins, specifically P-selectin and L-selectin [107]. Both P-selectin and L-selectin recognize platelet sulfatide, modulating platelet-platelet and platelet-leukocyte interactions, respectively. Also, P-selectin at the platelet surface associates with its putative ligand, P-selectin glycoprotein ligand-1 (PSGL-1), found on leukocyte (Figure 2), promoting platelet-leukocyte interactions. Thus, Dab2 exerts its inhibitory functions in both platelet homotypic and heterotypic interactions *via* sulfatide binding.

2.5.4 Dab2 SBM is the minimal sulfatide-binding unit of Dab2

A Dab2-derived peptide containing two sulfatide-binding motifs (SBMs, Figure 3A) has been designed and isolated by our group [108]. Structurally, a peptide representing the residues 24-58 of hDab2 SBM, shows a helical structure (Figure 3B) when embedded in dodecylphosphocholine (DPC) micelles [109], a membrane mimetic used to characterize membrane proteins by solution NMR spectroscopy. Dab2 SBM presents a disordered N-terminal region with two helices located at its

C-terminus. The membrane binding may induce a structural change of Dab2 SBM as its second helix maps to the longest β-strand of the natively folded PTB domain in a lipid-free form [41] (Figure 4). Paramagnetic NMR studies indicate that Dab2 SBM lies parallelly under the surface of sulfatide-loaded DPC micelles without crossing the hydrophobic core of the micelle. The helical region is believed to drive the peptide insertion into DPC micelles [109]. The major residues involved in sulfatide binding maps to the lysine residues (Lys49, Lys51, and Lys53) from the second sulfatide binding motif and three nonpolar residues (Ala52, Leu54, and Ile55). As expected, Dab2 SBM exhibits inhibitory platelet aggregation activity, similar to that determined for the RGDS (Arg-Gly-Asp-Ser) peptide derived from fibrinogen [109]. Consequently, Dab2 SBM is proposed as the minimal sulfatide-binding unit of Dab2 to function as an anti-aggregatory mediator of platelets [109].

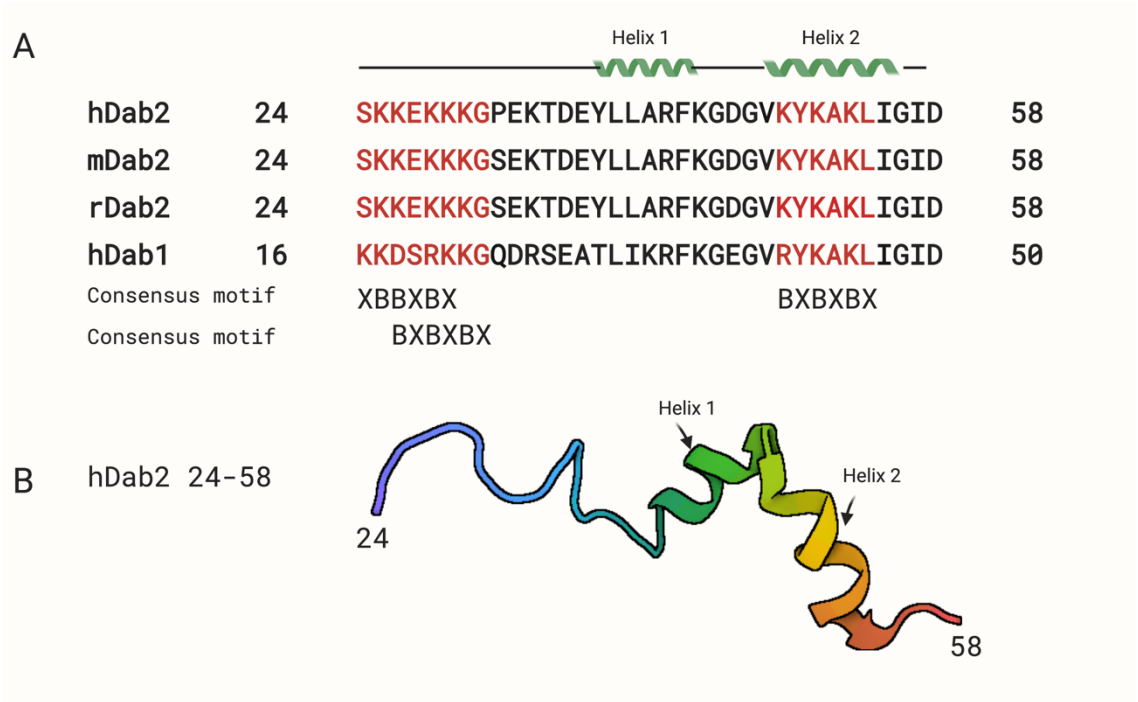

Figure 3. Schematic representation of conserved Dab2 SBM sequence and structure. (A) Sequence alignment of Dab2 SBM with secondary structure indicated on the top. Red residues are the two polybasic motifs. Consensus sulfatide-binding motifs are indicated at the bottom. X, any; B, basic. hDab2, *H. sapiens* Dab2; mDab2, *M. musculus* Dab2; rDab2, *R. norvegicus* Dab2; hDab1, *H. sapiens* Dab1. (B) The three-dimensional structure of hDab2 SBM (PDB 2LSW).

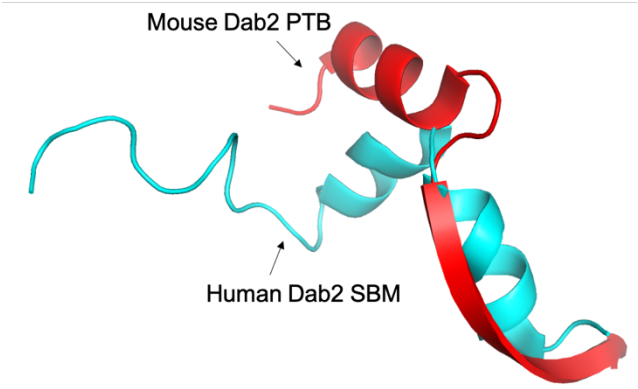

Figure 4. Superimposition of human Dab2 SBM and mouse Dab2 SBM region from the structure of the PTB domain. Human Dab2 SBM (24-58), PDB 2LSW. Mouse Dab2 PTB domain (PDB 1M7E) only shows residues 33-58, equivalent to human Dab2 SBM.

3. Application and research goals

Activated platelets express adhesion molecules and release numerous factors that enhance tumor-supportive microenvironment in circulation. P-selectin is a vital adhesion protein, present predominantly in platelets and endothelial cells. In platelets, P-selectin is present in α-granules under resting conditions. Within minutes after activation, P-selectin is exposed at the platelet surface resulting from α-granules fusing with the extracellular membrane. Hence, P-selectin is regarded as an established marker for platelet activation [110] and it is often increased in cancer cells [111]. On the platelet plasma membrane, P-selectin mediates tumor cells growth and metastasis by the rolling and tethering of CTCs to the blood vessel wall and the contribution to platelet-tumor cells aggregation which promote tumor cells adhesion to the endothelium.

The best-characterized ligands for P-selectin are PSGL-1 and the platelet glycoprotein GPIb in the GPI-IX-V complex. Both the ligands have abundant post-translational modifications required for receptor association and signal transmission, where sulfate regions consistently exists [112,113]. Consequently, sulfatide, a glycosphingolipid located at the surface of hemopoietic cells and certain tumor cells, is also found to bind to P-selectin. The discovery of this interaction can date back to 1991 when Aruffo *et al.* reported that sulfatide on the plasma membrane of granulates acted as a primary ligand of P-selectin on the tumor cells [114]. Since then, accumulative evidence have validated that sulfatides on the tumor cells are functional ligands of P-selectin in platelets, and such interaction facilitates the tumor cell metastatic progression [115–118]. Regardless of the current controversies regarding the expression level of sulfatides in different tumor types and cancer cell

lines, the elevation of sulfatides on the tumor cells is well supported by several lines of studies [29,92,119]. Given the presence of sulfatide and P-selectin on the tumor cell, it is likely that P-selectin-sulfatide interaction also assists in tumor cell interactions. However, there is no report targeting this aspect yet.

Also, sulfatide and P-selectin are both increasingly expressed and present on the plasma membrane of activated platelets. It has been observed that sulfatide recognition of P-selectin can further promote platelet activation and induce increased stability of platelet homogenous and heterogeneous aggregates, thereby triggering a positive feedback mechanism that potentiates the aggregates [120]. Given the role of platelet activation in cancer cell metastasis (discussed earlier), it is likely that sulfatide-P-selectin interaction between adjacent platelets can indirectly aid the tumor cell survival and growth by resulting in enhanced platelet activation. Taken together, P-selectin association with sulfatide occurs either between adjacent platelets or between platelets and tumor cells, both of which may directly or indirectly assist in tumor cell survival and growth. Therefore, the disruption of sulfatide binding to P-selectin provides a potential target to reduce the platelet-mediated cancer cell metastasis.

Dab2, an anticoagulant protein, is released from α-granules and mobilized to the extracellular membrane upon platelet activation. Of note, Dab2 can tightly control sulfatide-P-selectin interaction, which leads to a reduced P-selectin expression on activated platelets and inhibits the sulfatide-induced platelet aggregates when tested in microfluidic devices that mimic the shear stress levels of vein microcirculation [109]. Accordingly, a Dab2-derived peptide, Dab2 SBM, can reversibly bind to sulfatide with moderate affinity and reduce the number and size of sulfatide-induced platelet aggregates [109]. Therefore, Dab2 SBM-sulfatide interaction may impair the formation of platelet-tumor cells complex in several ways: (1) Dab2 SBM acts as a competitor of P-selectin for sulfatide binding, thus attenuating the platelet activation and aggregation, as well as the platelet adhesion to CTCs through P-selectin-sulfatide association. (2) The reduced platelet aggregates weaken platelets coating around CTCs, making CTCs exposed to the shear stress and the immune surveillance in circulation. (3) The reduced platelets activation results in decreased P-selectin expression, which may inhibit P-selectin mediated tumor growth [121]. Due to the transient

presence of Dab2 at the platelet surface, we proposed that Dab2 might be used at the site of solid tumors to inhibit the adhesion between platelets and CTCs without severely excessive bleeding.

Nevertheless, it is worthy of attention that Dab2 N-PTB (N terminal PTB domain) and Dab2 SBM exhibit different sulfatide binding affinity, with the former having a K_D at 0.6 μM and the latter ~50 μM. However, from a therapy perceptive, a Dab2 SBM-derived peptide (~4 kDa) bears many advantages over a protein drug derived from Dab2 N-PTB (~26 kDa). The manufacture and production of a therapeutic protein (MW >5 kDa) is a highly complicated process. A typical protein drug may require over 5,000 essential production procedures, which is ~10 folds greater than the production process of a small-molecule drug (MW <500 Da) [122]. Also, small-molecule drugs can readily enter inside cells and reach intracellular targets, and they have been successfully used to treat cancer patients by inhibiting oncoproteins [123]. On the other hand, the use of small-molecule drugs is limited by their size, which renders them unable to target and block the large surface area involved in protein-protein interactions. Meanwhile, a single mutation at the target site can cause drug deactivation, and a rapid development of cell resistance [124]. Peptide (500-5,000 Da) drugs combine the advantages of biological protein drugs and chemical small-molecule drugs. They can target large interface surfaces as specific as protein drugs and be able to cross the cell membrane and reach interior proteins as effectively as small-molecule drugs.

Therefore, this work aims to focus on characterizing the roles of residues within Dab2 SBM in sulfatides association from both structural and functional views. A residue screening will be applied by molecular docking studies, in which a model of Dab2 SBM binding to sulfatide will be proposed, and thus critical residues involved can be identified. Mutants with corresponding mutations will be constructed and their sulfatide binding capability will further be evaluated by multiple biophysical methods. Additionally, flow cytometry will be applied to determine the effects of each mutation on platelet activation in comparison with wild-type Dab2 SBM.

The resulting findings will help achieve a comprehensive understanding of Dab2 in its distinct roles in physiology and therapeutic potentials in pathophysiological processes. In the long run, we aim to develop a human-engineered Dab2 SBM-derived peptide with altered sulfatide-binding features, such as enhanced sulfatide binding affinity or selectivity. The development of such

engineered peptide could provide a potential new avenue of cancer therapy by mediating platelet activation, thereby alleviating platelet-mediated tumor metastasis.

References

1. Holinstat, M. Normal platelet function. *Cancer Metastasis Rev.* **36**, 195–198 (2017).
2. George, J. N. Platelets. *Lancet* **355**, 1531–1539 (2000).
3. Ghoshal, K. & Bhattacharyya, M. Overview of platelet physiology: Its hemostatic and nonhemostatic role in disease pathogenesis. *The Scientific World Journal* **2014**, (2014).
4. Machlus, K. R. & Italiano, J. E. The incredible journey: From megakaryocyte development to platelet formation. *Journal of Cell Biology* **201**, 785–796 (2013).
5. Holinstat, M. Normal platelet function. *Cancer Metastasis Rev.* **36**, 195–198 (2017).
6. JH, H. Platelet structure. *Platelets; Ed. by AD Michelson, Acad. Press* 37 (2002).
7. Blair, P. & Flaumenhaft, R. Platelet alpha-granules: basic biology and clinical correlates. *Blood Rev* **23**, 177–189 (2009).
8. Flaumenhaft, R. *Chapter 18. Platelet Secretion*. *Platelets* (2013). doi:10.1016/B978-0-12-387837-3.00018-3
9. Estevez, B. & Du, X. New concepts and mechanisms of platelet activation signaling. *Physiology* **32**, 162–177 (2017).
10. Eisinger, F., Patzelt, J. & Langer, H. F. The platelet response to tissue injury. *Frontiers in Medicine* **5**, 317 (2018).
11. Shattil, S. J., Kim, C. & Ginsberg, M. H. The final steps of integrin activation: The end game. *Nat. Rev. Mol. Cell Biol.* **11**, 288–300 (2010).
12. Brass, L. F., Newman, D. K., Wannermacher, K. M., Zhu, L. & Stalker, T. J. *Chapter 19. Signal Transduction During Platelet Plug Formation*. *Platelets* (2013). doi:10.1016/B978-0-12-387837-3.00019-5
13. Oury, C., Lecut, C., Hego, A., Wéra, O. & Delierneux, C. Purinergic control of inflammation and thrombosis: Role of P2X1 receptors. *Computational and Structural Biotechnology Journal* **13**, 106–110 (2015).
14. Huang, C.-L. *et al.* Disabled-2 is a novel alphaIIb-integrin-binding protein that negatively regulates platelet-fibrinogen interactions and platelet aggregation. *J. Cell Sci.* **119**, 4420–4430 (2006).

15. Rand, M. L. & Israels, S. J. Molecular Basis of Platelet Function. in *Hematology: Basic Principles and Practice* 1870-1884.e2 (Elsevier Inc., 2018). doi:10.1016/B978-0-323-35762-3.00125-6
16. Jin, J. & Kunapuli, S. P. Coactivation of two different G protein-coupled receptors is essential for ADP-induced platelet aggregation. *Proc. Natl. Acad. Sci. U. S. A.* **95**, 8070–8074 (1998).
17. Golebiewska, E. M. & Poole, A. W. Platelet secretion: From haemostasis to wound healing and beyond. *Blood Rev.* **29**, 153–162 (2015).
18. Fabre, J. E. *et al.* Decreased platelet aggregation, increased bleeding time and resistance to thromboembolism in P2Y1-deficient mice. *Nat. Med.* **5**, 1199–1202 (1999).
19. Daniel, J. L. *et al.* Molecular Basis for ADP-induced Platelet Activation. *J. Biol. Chem.* **273**, 2024–2029 (1998).
20. Zhang, Y. *et al.* Inhibition of platelet function using liposomal nanoparticles blocks tumor metastasis. *Theranostics* **7**, 1062–1071 (2017).
21. Tsuruo, T. & Fujita, N. Platelet aggregation in the formation of tumor metastasis. *Proc. Jpn. Acad. Ser. B. Phys. Biol. Sci.* **84**, 189–98 (2008).
22. Bambace, N. M. & Holmes, C. E. The platelet contribution to cancer progression. *J. Thromb. Haemost.* **9**, 237–249 (2011).
23. Medina, C. *et al.* Platelet aggregation-induced by caco-2 cells: Regulation by matrix metalloproteinase-2 and adenosine diphosphate. *J. Pharmacol. Exp. Ther.* **317**, 739–745 (2006).
24. Tesfamariam, B. Involvement of platelets in tumor cell metastasis. *Pharmacol. Ther.* **157**, 112–119 (2016).
25. Tsai, H.-J. & Tseng, C.-P. The adaptor protein Disabled-2: new insights into platelet biology and integrin signaling. *Thromb. J.* **14**, 28 (2016).
26. Zejuan Shenga Junqi Hea, Joseph A. Tuppend, W. David Martinc, Feng B. Dongd, Xiang-Xi Xub, E. R. S. Chromosomal location of murine Disabled-2 gene and structural comparison with its human ortholog. *Gene* **268**, 31–39 (2001).
27. Sheng, Z. *et al.* Chromosomal location of murine Disabled-2 gene and structural comparison with its human ortholog. *Gene* **268**, 31–39 (2001).
28. Xu, X. X., Yang, W., Jackowski, S. & Rock, C. O. Cloning of a novel phosphoprotein

regulated by colony-stimulating factor 1 shares a domain with the Drosophila disabled gene product. *Journal of Biological Chemistry* **271**, 14184–14191 (1995).

29. Mok, S. C. *et al.* Molecular cloning of differentially expressed genes in human epithelial ovarian cancer. *Gynecol. Oncol.* **52**, 247–252 (1994).
30. Chetrit, D., Ziv, N. & Ehrlich, M. Dab2 regulates clathrin assembly and cell spreading. *Biochem. J.* **418**, 701–715 (2009).
31. Maurer, M. E. & Cooper, J. A. Endocytosis of megalin by visceral endoderm cells requires the Dab2 adaptor protein. *J. Cell Sci.* **118**, 5345–5355 (2005).
32. Kim, J. A., Bae, S. H., Choi, Y. J., Kim, K. H. & Park, S. S. Feed-back regulation of disabled-2 (Dab2) p96 isoform for GATA-4 during differentiation of F9 cells. *Biochem. Biophys. Res. Commun.* **421**, 591–598 (2012).
33. Zuber, J. *et al.* A genome-wide survey of RAS transformation targets. *Nat. Genet.* **24**, 144–152 (2000).
34. Karam, J. A. *et al.* Decreased DOC-2/DAB2 expression in urothelial carcinoma of the bladder. *Clin. Cancer Res.* **13**, 4400–4406 (2007).
35. Tseng, C. P. *et al.* Disabled-2 small interfering RNA modulates cellular adhesive function and MAPK activity during megakaryocytic differentiation of K562 cells. *FEBS Lett.* **541**, 21–27 (2003).
36. Tao, W., Moore, R., Smith, E. R. & Xu, X. X. Endocytosis and physiology: Insights from disabled-2 deficient mice. *Front. Cell Dev. Biol.* **4**, 1–11 (2016).
37. Moore, R., Cai, K. Q., Tao, W., Smith, E. R. & Xu, X. X. Differential requirement for Dab2 in the development of embryonic and extra-embryonic tissues. *BMC Dev. Biol.* **13**, 1–15 (2013).
38. Tao, W., Moore, R., Meng, Y., Smith, E. R. & Xu, X. X. Endocytic adaptors Arh and Dab2 control homeostasis of circulatory cholesterol. *J. Lipid Res.* **57**, 809–817 (2016).
39. van der Geer, P. & Pawson, T. The PTB domain: a new protein module implicated in signal transduction. *Trends Biochem. Sci.* **20**, 277–280 (1995).
40. Stolt, P. C., Vardar, D. & Blacklow, S. C. The dual-function disabled-1 PTB domain exhibits site independence in binding phosphoinositide and peptide ligands. *Biochemistry* **43**, 10979–10987 (2004).
41. Finkielstein, C. V. & Capelluto, D. G. S. Disabled-2: A modular scaffold protein with

multifaceted functions in signaling. *BioEssays* **38**, S45–S55 (2016).

42. Maurer, M. E. & Cooper, J. A. The adaptor protein Dab2 sorts LDL receptors into coated pits independently of AP-2 and ARH. *J. Cell Sci.* **119**, 4235–4246 (2006).
43. Kaksonen, M. & Roux, A. Mechanisms of clathrin-mediated endocytosis. *Nat. Rev. Mol. Cell Biol.* **19**, 313–326 (2018).
44. Morris, S. M. & Cooper, J. A. Disabled-2 colocalizes with the LDLR in clathrin-coated pits and interacts with AP-2. *Traffic* **2**, 111–123 (2001).
45. Mishra, S. K. *et al.* Disabled-2 exhibits the properties of a cargo-selective endocytic clathrin adaptor. *EMBO J.* **21**, 4915–4926 (2002).
46. Owen, D. J. *et al.* A structural explanation for the binding of multiple ligands by the α-adaptin appendage domain. *Cell* **97**, 805–815 (1999).
47. Mulkearns, E. E. & Cooper, J. A. FCH domain only-2 organizes clathrin-coated structures and interacts with Disabled-2 for low-density lipoprotein receptor endocytosis. *Mol. Biol. Cell* **23**, 1330–1342 (2012).
48. Teckchandani, A., Mulkearns, E. E., Randolph, T. W., Toida, N. & Cooper, J. A. The clathrin adaptor Dab2 recruits EH domain scaffold proteins to regulate integrin β1 endocytosis. *Mol. Biol. Cell* **23**, 2905–2916 (2012).
49. Morris, S. M. *et al.* Myosin VI binds to and localises with Dab2, potentially linking receptor-mediated endocytosis and the actin cytoskeleton. *Traffic* **3**, 331–341 (2002).
50. Zhou, J., Scholes, J. & Hsieh, J. T. Characterization of a novel negative regulator (DOC-2/DAB2) of c-Src in normal prostatic epithelium and cancer. *J. Biol. Chem.* **278**, 6936–6941 (2003).
51. Spudich, G. *et al.* Myosin VI targeting to clathrin-coated structures and dimerization is mediated by binding to Disabled-2 and PtdIns(4,5)P2. *Nat. Cell Biol.* **9**, 176–183 (2007).
52. Fazili, Z., Sun, W., Mittelstaedt, S., Cohen, C. & Xu, X. X. Disabled-2 inactivation is an early step in ovarian tumorigenicity. *Oncogene* **18**, 3104–3113 (1999).
53. Schwahn, D. J. & Medina, D. p96, a MAPK-related protein, is consistently downregulated during mouse mammary carcinogenesis. *Oncogene* **17**, 1173–1178 (1998).
54. Xu, H.-T. *et al.* Disabled-2 and Axin are concurrently colocalized and underexpressed in lung cancers. *Hum. Pathol.* **42**, 1491–1498 (2011).
55. Kleeff, J. *et al.* Down-regulation of DOC-2 in colorectal cancer points to its role as a tumor

suppressor in this malignancy. *Dis. Colon Rectum* **45**, 1242–1248 (2002).

56. Ogbu, S. C. *et al.* The role of disabled-2 (Dab2) in diseases. *Gene* 145202 (2020). doi:10.1016/j.gene.2020.145202
57. Hocevar, B. A. Loss of Disabled-2 Expression in Pancreatic Cancer Progression. *Sci. Rep.* **9**, 1–11 (2019).
58. Zhang, Z., Chen, Y., Xie, X. & Tang, J. J. The expression of disabled-2 is common reduced in meningiomas. *Neurol. India* **62**, 57–61 (2014).
59. Kumar Anupam, Chatopadhyay Tusharkant, Siddhartha Datta Gupta, R. R. & Kumar. Loss of disabled-2 expression is an early event in esophageal squamous tumorigenesis. *World J Gastroenterol* **12**, 6041–6043 (2006).
60. Vuong, N. H., Salah Salah, O. & Vanderhyden, B. C. 17β-Estradiol sensitizes ovarian surface epithelium to transformation by suppressing Disabled-2 expression /631/67/1517/1709 /631/80/304 /631/443/494/2732/2730 /13 /13/51 /13/106 /14/19 /14/63 /38 /38/61 /38/109 /64 /64/60 /82/1 article. *Sci. Rep.* **7**, 1–12 (2017).
61. Potdar, P. & Lotey, N. Role of circulating tumor cells in future diagnosis and therapy of cancer. *J. Cancer Metastasis Treat.* **1**, 44 (2015).
62. Prunier, C., Hocevar, B. A. & Howe, P. H. Wnt signaling: Physiology and pathology. *Growth Factors* **22**, 141–150 (2004).
63. Lustig, B. & Behrens, J. The Wnt signaling pathway and its role in tumor development. *Journal of Cancer Research and Clinical Oncology* **129**, 199–221 (2003).
64. Yue, J. Abstract 4184: Genetic and pharmacological disruption of survivin suppressed primary and metastatic tumor growth by attenuating TGFB pathway in ovarian cancer. in *Cancer Research* **80**, 4184–4184 (American Association for Cancer Research (AACR), 2020).
65. Lähde, M. *et al.* Expression of R-spondin1 in Apc Mice Reduces Growth of Intestinal Adenomas by Altering Wnt and TGFB Signaling. *Gastroenterology* (2020). doi:10.1053/j.gastro.2020.09.011
66. Xie, Y. *et al.* Disabled homolog 2 is required for migration and invasion of prostate cancer cells. *Front. Med.* **9**, 312–321 (2015).
67. Xie, X. M. *et al.* Aberrant hypermethylation and reduced expression of disabled-2 promote the development of lung cancers. *Int. J. Oncol.* **43**, 1636–1642 (2013).

68. Prunier, C. & Howe, P. H. Disabled-2 (Dab2) is required for transforming growth factor β-induced epithelial to mesenchymal transition (EMT). *J. Biol. Chem.* **280**, 17540–17548 (2005).
69. Itami, Y. *et al.* Disabled homolog 2 (DAB2) protein in tumor microenvironment correlates with aggressive phenotype in human urothelial carcinoma of the bladder. *Diagnostics* **10**, (2020).
70. Cho, S. Y., Cho, S. Y., Lee, S. H. & Park, S. S. Differential expression of mouse Disabled 2 gene in retinoic acid-treated F9 embryonal carcinoma cells and early mouse embryos. *Mol. Cells* **9**, 179–184 (1999).
71. Martin, J. C., Herbert, B. S. & Hocevar, B. A. Disabled-2 downregulation promotes epithelial-to-mesenchymal transition. *Br. J. Cancer* **103**, 1716–1723 (2010).
72. Vázquez-Carretero, M. D., García-Miranda, P., Calonge, M. L., Peral, M. J. & Ilundáin, A. A. Regulation of Dab2 expression in intestinal and renal epithelia by development. *J. Cell. Biochem.* **112**, 354–361 (2011).
73. Chao, A. *et al.* Regulation of ovarian cancer progression by microRNA-187 through targeting Disabled homolog-2. *Oncogene* **31**, 764–775 (2012).
74. Chaudhury, A. *et al.* TGF-B-mediated phosphorylation of hnRNP E1 induces EMT via transcript-selective translational induction of Dab2 and ILEI. *Nat. Cell Biol.* **12**, 286–293 (2010).
75. Huang, C. L. *et al.* Disabled-2 is a negative regulator of integrin αIIbβ3-mediated fibrinogen adhesion and cell signaling. *J. Biol. Chem.* **279**, 42279–42289 (2004).
76. Ambrosio, A. L. & Di Pietro, S. M. Mechanism of platelet a-granule biogenesis: Study of cargo transport and the VPS33B-VPS16B complex in a model system. *Blood Adv.* **3**, 2617–2626 (2019).
77. Ambrosio, A. L., Boyle, J. A. & Di Pietro, S. M. Mechanism of platelet dense granule biogenesis: Study of cargo transport and function of Rab32 and Rab38 in a model system. *Blood* **120**, 4072–4081 (2012).
78. Tsai, H. J. *et al.* Disabled-2 is required for efficient hemostasis and platelet activation by thrombin in mice. *Arterioscler. Thromb. Vasc. Biol.* **34**, 2404–2412 (2014).
79. Wagner, C. L. *et al.* Analysis of GPIIb/IIIa receptor number by quantification of 7E3 binding to human platelets. *Blood* **88**, 907–914 (1996).

80. Li, Z., Delaney, M. K., O'Brien, K. A. & Du, X. Signaling during platelet adhesion and activation. *Arterioscler. Thromb. Vasc. Biol.* **30**, 2341–2349 (2010).
81. Shattil, S. J. Signaling through platelet integrin αIIbβ3: Inside-out, outside-in, and sideways. in *Thrombosis and Haemostasis* **82**, 318–325 (Schattauer GmbH, 1999).
82. Hung, W. S. *et al.* The endocytic adaptor protein Disabled-2 is required for cellular uptake of fibrinogen. *Biochim. Biophys. Acta - Mol. Cell Res.* **1823**, 1778–1788 (2012).
83. Calderwood, D. A. *et al.* Integrin β cytoplasmic domain interactions with phosphotyrosine-binding domains: A structural prototype for diversity in integrin signaling. *Proc. Natl. Acad. Sci. U. S. A.* **100**, 2272–2277 (2003).
84. Tsai, H. J. *et al.* Functional links between Disabled-2 Ser723 phosphorylation and thrombin signaling in human platelets. *J. Thromb. Haemost.* **15**, 2029–2044 (2017).
85. Rozenvayn, N. & Flaumenhaft, R. Phosphatidylinositol 4,5-bisphosphate mediates Ca2+-induced platelet α-granule secretion. Evidence for type II phosphatidylinositol 5-phosphate 4-kinase function. *J. Biol. Chem.* **276**, 22410–22419 (2001).
86. Racaud-Sultan, C. *et al.* Rapid and transient thrombin stimulation of phosphatidylinositol 4,5-bisphosphate synthesis but not of phosphatidylinositol 3,4-bisphosphate independent of phospholipase C activation in platelets. *FEBS Lett.* **330**, 347–351 (1993).
87. Drahos, K. E., Welsh, J. D., Finkielstein, C. V & Capelluto, D. G. S. Sulfatides partition disabled-2 in response to platelet activation. *PLoS One* **4**, (2009).
88. Sánchez-Cortés, J. & Mrksich, M. The Platelet Integrin αIIbβ3 Binds to the RGD and AGD Motifs in Fibrinogen. *Chem. Biol.* **16**, 990–1000 (2009).
89. Honke, K. *et al.* Molecular cloning and expression of cDNA encoding human 3'-phosphoadenylylsulfate:galactosylceramide 3'-sulfotransferase. *J. Biol. Chem.* **272**, 4864–4868 (1997).
90. Burkartf, T., Caimig, L., Siegristf, H. P., Herschkowitzf, N. N. & Wiesmannf, U. N. *Vesicular Transport of Sulfatide in the Myelinating Mouse Brain FUNCTIONAL ASSOCIATION WITH LYSOSOMES?*. THE JOURNAL OF BIOLOGICAL CHEMISTRY* **257**, (1982).
91. Guchhait, P., Shrimpton, C., Honke, K., Thiagarajan, P. & Lopez, J. A. A Critical Role for Membrane Sulfatide in Platelet Aggregation. *Blood* **104**, 626–626 (2004).
92. Takahashi, T. & Suzuki, T. Role of sulfatide in normal and pathological cells and tissues. *J.*

Lipid Res. **53**, 1437–1450 (2012).

93. Kushi, Y. *et al.* Sulfatide is expressed in both erythrocytes and platelets of bovine origin. *Biochim. Biophys. Acta - Lipids Lipid Metab.* **1304**, 254–262 (1996).
94. Borthakur, G. *et al.* Sulfatides inhibit platelet adhesion to von Willebrand factor in flowing blood. *J. Thromb. Haemost.* **1**, 1288–1295 (2003).
95. Merten, M. & Thiagarajan, P. Role for Sulfatides in Platelet Aggregation. *Circulation* **104**, 2955–2960 (2001).
96. Roberts, D. D. *et al.* Laminin binds specifically to sulfated glycolipids. *Proc. Natl. Acad. Sci. U. S. A.* **82**, 1306–1310 (1985).
97. Roberts, D. D. *et al. THE JOURNAL OF BIOLOGICAL CHEMISTRY The Platelet Glycoprotein Thrombospondin Binds Specifically to Sulfated Glycolipids**. **260**, (1985).
98. Ding, Z., Kawashima, H. & Miyasaka, M. *Sulfatide binding and activation of leukocytes through an L-selectin-independent pathway*.
99. Schousboe, I. & Rasmussen, M. S. The effect of β2-glycoprotein i on the dextran sulfate and sulfatide activation of the contact system (Hageman factor system) in the blood coagulation. *Int. J. Biochem.* **20**, 787–792 (1988).
100. Merten, M. & Thiagarajan, P. Role for sulfatides in platelet aggregation. *Circulation* **104**, 2955–2960 (2001).
101. Merten, M. *et al.* Sulfatides activate platelets through P-selectin and enhance platelet and platelet-leukocyte aggregation. *Arterioscler. Thromb. Vasc. Biol.* **25**, 258–263 (2005).
102. Ishizuka, I. Chemistry and functional distribution of sulfoglycolipids. *Progress in Lipid Research* **36**, 245–319 (1997).
103. Chetrit, D., Ziv, N. & Ehrlich, M. Dab2 regulates clathrin assembly and cell spreading. *Biochem. J.* **418**, 701–715 (2009).
104. Simonis, D., Schlesinger, M., Seelandt, C., Borsig, L. & Bendas, G. Analysis of SM4 sulfatide as a P-selectin ligand using model membranes. *Biophys. Chem.* **150**, 98–104 (2010).
105. Kwiatkowska, K. One lipid, multiple functions: How various pools of PI(4,5)P2 are created in the plasma membrane. *Cellular and Molecular Life Sciences* **67**, 3927–3946 (2010).
106. Alajlouni, R., Drahos, K. E., Finkielstein, C. V. & Capelluto, D. G. S. Lipid-mediated membrane binding properties of Disabled-2. *Biochim. Biophys. Acta - Biomembr.* **1808**,

2734–2744 (2011).

107. Capelluto, D. G. S. *Lipid-mediated Protein Signaling*. **991**, (2013).

108. Xiao, S., Zhao, X., Finkielstein, C. V. & Capelluto, D. G. S. A rapid procedure to isolate isotopically labeled peptides for NMR studies: Application to the Disabled-2 sulfatide-binding motif. *J. Pept. Sci.* **20**, 216–222 (2014).

109. Xiao, S. *et al.* Structure, Sulfatide Binding Properties, and Inhibition of Platelet Aggregation by a Disabled-2 Protein-derived Peptide. *J. Biol. Chem.* **287**, 37691–37702 (2012).

110. Vinik, A. I., Erbas, T., Sun Park, T., Nolan, R. & Pittenger, G. L. Platelet dysfunction in type 2 diabetes. *Diabetes Care* **24**, 1476–1485 (2001).

111. Mezouar, S. *et al.* Role of platelets in cancer and cancer-associated thrombosis: Experimental and clinical evidences. *Thrombosis Research* (2016). doi:10.1016/j.thromres.2016.01.006

112. Pouyani, T. & Seed, B. PSGL-1 recognition of P-selectin is controlled by a tyrosine sulfation consensus at the PSGL-1 amino terminus. *Cell* **83**, 333–343 (1995).

113. Romo, G. M. *et al.* The glycoprotein Ib-IX-V complex is a platelet counterreceptor for P-selectin. *J. Exp. Med.* **190**, 803–813 (1999).

114. Aruffo, A., Kolanus, W., Walz, G., Fredman, P. & Seed, B. CD62/P-selectin recognition of myeloid and tumor cell sulfatides. *Cell* **67**, 35–44 (1991).

115. Suchanski, J. *et al.* Sulfatide decreases the resistance to stress-induced apoptosis and increases P-selectin-mediated adhesion: A two-edged sword in breast cancer progression. *Breast Cancer Res.* **20**, 133 (2018).

116. Garcia, J., Callewaert, N. & Borsig, L. P-selectin mediates metastatic progression through binding to sulfatides on tumor cells. *Glycobiology* **17**, 185–196 (2007).

117. Simonis, D., Schlesinger, M., Seelandt, C., Borsig, L. & Bendas, G. Analysis of SM4 sulfatide as a P-selectin ligand using model membranes. *Biophys. Chem.* **150**, 98–104 (2010).

118. Bajorath, J. *et al.* CD62/P-Selectin Binding Sites for Myeloid Cells and Sulfatides Are Overlapping. *Biochemistry* **33**, 1332–1339 (1994).

119. Liu, Y. *et al.* Elevation of sulfatides in ovarian cancer: An integrated transcriptomic and lipidomic analysis including tissue-imaging mass spectrometry. *Mol. Cancer* **9**, (2010).

120. Merten, M. *et al.* Sulfatides activate platelets through P-selectin and enhance platelet and

platelet-leukocyte aggregation. *Arterioscler. Thromb. Vasc. Biol.* **25**, 258–263 (2005).

121. Qi, C. *et al.* P-selectin-mediated adhesion between platelets and tumor cells promotes intestinal tumorigenesis in $Apc^{min/+}$ mice. *Int. J. Biol. Sci.* **11**, 679–687 (2015).
122. Kimchi-Sarfaty, C. *et al.* Building better drugs: Developing and regulating engineered therapeutic proteins. *Trends in Pharmacological Sciences* **34**, 534–548 (2013).
123. Sauna, Z. E. *et al.* Recent advances in (therapeutic protein) drug development. *F1000Research* **6**, (2017).
124. Sorolla, A. *et al.* Precision medicine by designer interference peptides: applications in oncology and molecular therapeutics. *Oncogene* **39**, 1167–1184 (2020).

Chapter 2 Structural, in silico, and functional analysis of a Disabled-2-derived peptide for recognition of sulfatides

Wei Song [a], Carter J. Gottschalk [b], Tuo-Xian Tang [a], Andrew Biscardi [a], Jeffrey F. Ellena [c] Carla V. Finkielstein [d], Anne M. Brown [b], and Daniel G. S. Capelluto [a,*]

[a] Protein Signaling Domains Laboratory, Department of Biological Sciences, Fralin Life Sciences Institute, and Center for Soft Matter and Biological Physics, Virginia Tech, Blacksburg, VA 24061, United States; [b] Research and Informatics, University Libraries, Biochemistry Department, and Center for Drug Discovery, Virginia Tech, Blacksburg, VA, United States; [c] Biomolecular Magnetic Resonance Facility, University of Virginia, Charlottesville VA, 22904, United States; [d] Integrated Cellular Responses Laboratory, Department of Biological Sciences, Fralin Biomedical Institute, and Center for Drug Discovery, Virginia Tech Carilion, Roanoke, VA 24016, United States.

Authorship Attribution

W.S., C.V.F., A.M.B., and D.G.S.C. conceived the experiments. C.J.G. and A.M.B performed, processed, and visualized molecular docking. W.S., T.X.T., and A.M.B. purified proteins and performed lipid-protein overlay assays. W.S. performed and analyzed CD and SPR experiments. J.F.E. collected, processed, and visualized NMR data. W.S. and C.V.F. designed the flow cytometry experiments. W.S. performed and analyzed the flow cytometry experiments. D.G.S.C. analyzed experimental data and wrote the manuscript with all authors contributing to the edition of the manuscript.

As published in ***Scientific Reports****:*

Song, W., Gottschalk, C.J., Tang, TX. et al. Structural, in silico, and functional analysis of a Disabled-2-derived peptide for recognition of sulfatides. Sci Rep 10, 13520 (2020). https://doi.org/10.1038/s41598-020-70478-0

Abstract

Disabled-2 (Dab2) is an adaptor protein that regulates the extent of platelet aggregation by two mechanisms. In the first mechanism, Dab2 intracellularly downregulates the integrin $\alpha_{IIb}\beta_3$ receptor, converting it to a low affinity state for adhesion and aggregation processes. In the second mechanism, Dab2 is released extracellularly and interacts with the pro-aggregatory mediators, the integrin $\alpha_{IIb}\beta_3$ receptor and sulfatides, blocking their association to fibrinogen and P-selectin, respectively. Our previous research indicated that a 35-amino acid region within Dab2, which we refer to as the sulfatide-binding peptide (SBP), contains two potential sulfatide-binding motifs represented by two consecutive polybasic regions. Using molecular docking, nuclear magnetic resonance, lipid-binding assays, and surface plasmon resonance, this work identifies the critical Dab2 residues within SBP that are responsible for sulfatide binding. Molecular docking suggested that a hydrophilic region, primarily mediated by R42, is responsible for interaction with the sulfatide headgroup, whereas the C-terminal polybasic region contributes to interactions with acyl chains. Furthermore, we demonstrated that, in Dab2 SBP, R42 significantly contributes to the inhibition of platelet P-selectin surface expression. The Dab2 SBP residues that interact with sulfatides resemble those described for sphingolipid-binding in other proteins, suggesting that sulfatide-binding proteins share common binding mechanisms.

Keywords: Disabled-2; sulfatide; liposome; platelets; molecular docking; surface plasmon resonance; integrin receptor.

Introduction

The adaptor protein Disabled-2 (Dab2) is a multimodular signaling molecule involved in various cellular functions including protein trafficking, cell growth and differentiation, cell adhesion, and modulation of platelet aggregation [1]. Two Dab orthologs, Dab1 and Dab2, are present in mammals. Dab1 is predominantly expressed in the brain [2], whereas Dab2 is ubiquitously expressed in different tissues [3,4]. Dab2 expression levels have been reported to exhibit a significant effect on cancer initiation and progression. Indeed, Dab2 expression is lost in breast, ovarian, prostate [5], bladder [6], and colorectal cancer cells [7], suggesting that Dab2 can act as a tumor suppressor [8]. Two alternative spliced forms of Dab2 are expressed in humans, p96 and p67, with the latter lacking a central exon [3]. Dab2 contains a phosphotyrosine-binding (PTB) domain located at the N-terminus, clathrin-binding sites, NPF and DPF motifs, and a proline-rich SH3 domain located at the C-terminus, indicating that Dab2 primarily functions as an adaptor protein.

Recently, Dab2 was characterized as a negative regulator of platelet aggregation by modulating both pro-aggregatory inside-out and outside-in signaling pathways [1]. Modulation of inside-out signaling by Dab2 is mediated by its cytosolic S24-phosphorylated form, which recognizes the β3 subunit of $\alpha_{IIb}\beta_3$ integrin, downregulating fibrinogen-mediated adhesion [9]. In outside-in signaling, ligand-receptor complexes on activated platelets promote platelet spreading, granule secretion, stabilization of the adhesion and aggregation of platelets, and clot retraction [10]. Some of the components of the intracellular granules are required to limit the extent of platelet activation, adhesion, and aggregation. Platelet function must be tightly modulated, as uncontrolled platelet activation can trigger unwanted clinical complications such as thrombocytopenia and thrombosis [11]. Dab2 is released from α-granules and relocates to the platelet surface where it modulates outside-in signaling [12]. To do this, Dab2 presents two extracellular targets. At the extracellular membrane of platelet, Dab2 associates with the α_{IIb} subunit of integrin *via* its RGD motif, preventing integrin-fibrinogen interactions. Dab2 also binds to sulfatides [13], a class of negatively charged sphingolipids found on most eukaryotic cell surfaces [14]. Interestingly, cleavage of Dab2 by the platelet agonist thrombin may be prevented when Dab2 is associated with the sphingolipid [13]. Binding of Dab2 to sulfatides limits P-selectin association to sulfatides [15], which is required to prolong platelet aggregation [16].

Initial studies reported that Dab2 binds sulfatides at its N-terminus including the PTB domain (N-PTB; residues 1-241 in hDab2) [13]. Combined mutations in residues K25, K49, K51, and K53 markedly reduce sulfatide binding and platelet aggregation. Further studies showed that an α-helical-rich region of 35 amino acids within the Dab2 N-PTB, which was predicted to contain two potential sulfatide-binding motifs (referred to as the sulfatide-binding peptide, SBP), mimic the inhibitory platelet-platelet interaction effects of Dab2 N-PTB [17]. In this report, by using a combination of structural, molecular docking, and functional approaches, we refined the mode by which SBP, the minimal sulfatide-binding unit derived from Dab2, associates with sulfatides. Molecular docking showed that the Dab2 SBP residues around α-helix 1 are required for interactions with the sulfatide head group, whereas helix 2 mediates sulfatide acyl chain interactions. Furthermore, we predict that R42, located in the first α-helix of Dab2 SBP, forms hydrogen bonds with the OS atoms of the sulfate group in the sulfatide. We demonstrate that both the charge and stereochemistry of R42 is critical for Dab2 SBP's sulfatide recognition and inhibition of platelet P-selectin surface expression. Results from this report provide details of how Dab2 interacts with sulfatides, which can be used for the design of a Dab2-derived peptide that can block sulfatide interactions, and, consequently, prevent undesired platelet aggregation events.

Results

Refining the sulfatide-binding site in Dab2 SBP

Previous NMR studies showed that the last 20 residues of Dab2 SBP, with a C-terminal polybasic region 49-KYKAKL-54 (**Fig. 1a**), plays a major role in sulfatide interactions [17]. Molecular docking was performed to refine potential residue interactions between a single sulfatide molecule and the model of the DPC-bound structural conformation of Dab2 SBP (PDB ID: 2LSW) containing vector residues (19-GPLGS-23), which were added to the N-terminus to match the experimental peptide used in this work. After energy minimization, the structure of Dab2 SBP was validated and showed favorable energetics and side chain positioning using Ramachandran plots, ProSA and QMEAN analyses (Supplementary **Fig. S1**). All nine docking poses hit a similar Dab2 SBP scaffold and indicated that the P32 (backbone), K30 (backbone), and R42 residues form hydrogen bonds with the OS atoms of the sulfate group in the sulfatide, whereas the acyl chains faced the α-helix 2 of the peptide (**Fig. 1b-c**). Specifically, the side chain of R42 interacted with the sulfatide head group forming hydrogen bonds and electrostatic interactions that were

approximately 3Å apart (**Fig. 1c**). Both E33 and Y38 interacted with the galactose moiety (**Fig. 1c**). The conserved 49-KYKAKL-54 region in Dab2 SBP (**Fig. 1a**) was initially suggested to provide an electrostatic environment to attract and accommodate the negatively charged sulfatide in its Dab2 SBP binding pocket [17]. However, molecular docking results showed a strong R42 interaction with the sulfate head group, which led to consistent positioning of the sulfatide acyl tails towards α-helix 2. Initial docking results and fingerprinting showed that the CH2 moieties of the K49 and K51 residues interacted with the acyl tails. As K49 and K51 are critical for sulfatide binding [13], the docking results suggest that the four CH2 moieties in K49 and K51 contribute to a hydrophobic

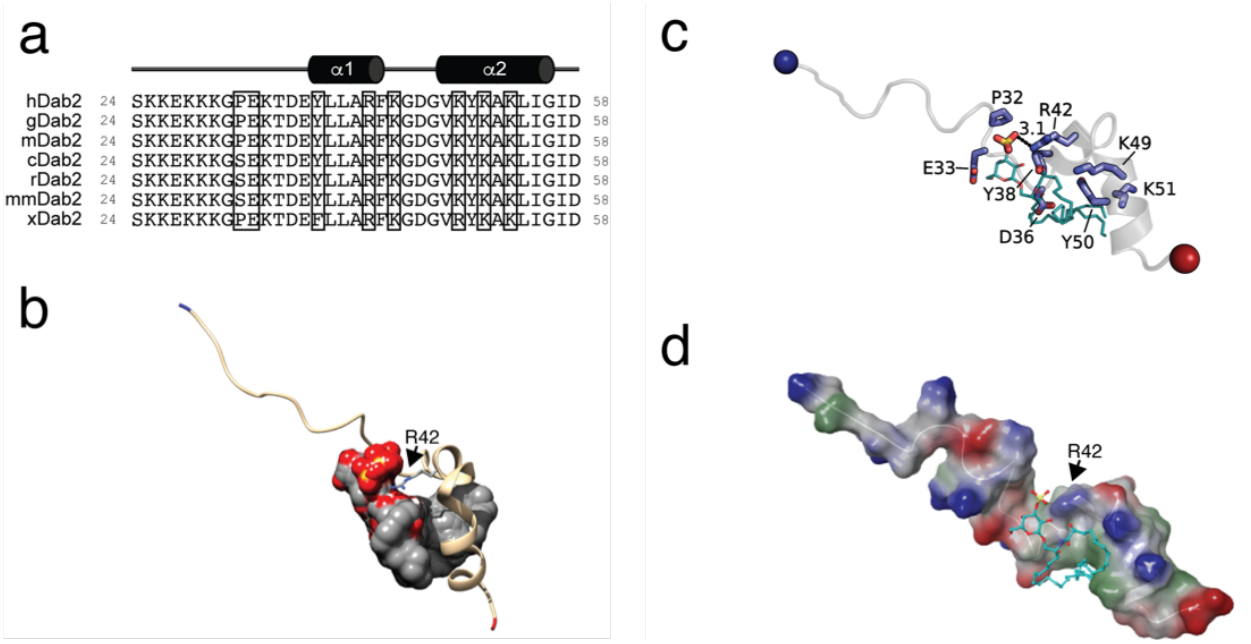

Figure 1. Sulfatide docking onto Dab2 SBP. (**a**) Sequences of the closest homologues of Dab2 proteins corresponding to the SBP region. hDab2, *Homo sapiens* Dab2; gDab2, *Gorilla gorilla* Dab2; mDab2, *Mandrillus leucopheous* Dab2; cDab2, *Canis lupus familiaris* Dab2; rDab2, *Rattus norvegicus* Dab2; mmDab2, *Mus musculus* Dab2; xDab2, *Xenopus laevis* Dab2. Residues implicated in sulfatide binding, as determined from this work, are boxed. (**b**) Overlaid poses of sulfatide docked to Dab2 SBP. Dab2 SBP is rendered as a cartoon and is colored tan with the N-terminus colored blue and the C-terminus colored red. R42 is shown as a stick that is colored gray and by atom type. The nine poses produced by AutoDock Vina are shown as a gray surface and by atom type. The side chain of R42 is a blue colored stick. Sulfatides (cyan) are shown as sticks and colored by element. (**c**) Key sulfatide-binding residues of Dab2. Dab2 SBP is rendered as a cartoon colored a transparent gray with the N- and C-terminus shown as blue and red spheres, respectively. Key residues are shown as blue sticks and labelled. (**d**) Surface representation of

sulfatide-bound Dab2 SBP showing the hydrophobic (green), positively charged (blue), and negatively charged (red) surface regions. The sulfatide backbone is represented as a stick colored with carbon as cyan, sulfate as yellow, and oxygen as red. Surface potential was calculated using Schrodinger Maestro.

pocket (**Fig. 1d**) in α-helix 2 of Dab2 SBP and aid in accommodating acyl tails, leading to more energetically favorable positioning of the sulfate head group towards R42 (Supplementary **Table S1**). Hydrophobic interactions in α-helix 2 were also provided by the Dab2 SBP residues Y50, L54, and I55 (**Fig. 1c** and Supplementary **Table S1**). Altogether, molecular docking data indicate that α-helix 1 of Dab2 SBP is involved in contacts with the sulfatide head group, whereas α-helix 2 favors hydrophobic contacts with the acyl chains of the lipid.

Conformational flexibility of Dab2 SBP upon sulfatide binding

In agreement with our previous work [17], the addition of DPC-embedded sulfatide to DPC-containing Dab2 SBP has little or no effect on ^{1}H and ^{15}N chemical shifts of residues S24-E37 but perturbs resonances of most of the residues spanning residues Y38 to D58 (Supplementary **Fig. S2**). The heights of HSQC peaks for residues E33-I56 are considerably lower than those for residues S24-G31 for both DPC-containing Dab2 SBP with and without sulfatide-embedded micelles (Supplementary **Fig. S2**). Residues S24-G31 likely do not contact DPC micelles and are highly mobile and solvent-exposed as suggested from paramagnetic relaxation experiments [17]. Residues Y38-I55, on the other hand, contribute to the secondary structure in Dab2 SBP and strongly interact with DPC micelles [17]. Consequently, as observed in Supplementary **Fig. S2**, residues E33-I56 may be poorly observable with solution NMR when Dab2 SBP is bound to either sulfatide-free or -embedded DPC micelles.

We also used NMR to characterize the backbone dynamics of Dab2 SBP in its free-and sulfatide-bound states. Picosecond to nanosecond backbone dynamics, measured by $^{1}H–^{15}N$, heteronuclear Overhauser effect (NOE) of DPC-associated Dab2 SBP, showed very flexible N- and C-termini

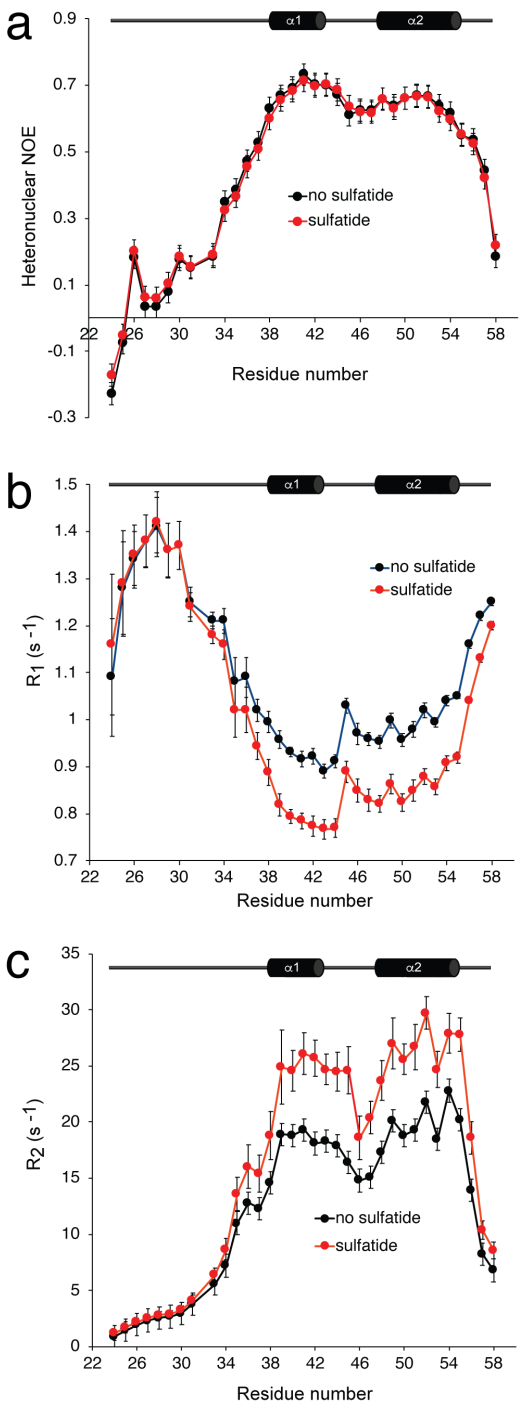

Figure 2. Dab2 SBP dynamics characterized by NMR relaxation measurements. $^{1}H–^{15}N$ NOE ratio (**a**), longitudinal relaxation rates, R_1 (**b**), and transversal relaxation rates, R_2 (**c**) of DPC-embedded Dab2 SBP in the absence (black) or presence (red) of 8-fold DPC-embedded sulfatides. The secondary structure of Dab2 SBP is depicted at the top of each panel.

and a rigid structure spanning residues E37-I56; such flexibility was not altered by sulfatides (**Supplementary Fig. S2**). Addition of sulfatides decreased R_1 and increased R_2 of residues T35-I56. The relaxation data indicates that sulfatide has little or no effect on the motions of residues S24-G31 but shifts the spectral density of residues T35-I56 to a lower frequency. This could be due to sulfatide binding to residues T35-I56, consistent with the data from both molecular docking (**Fig. 1b-c**) and HSQC titrations of the peptide with the lipid (**Fig. 2a, b**), or a sulfatide-induced increase in DPC micelle size or both.

In silico and lipid-binding assays of Dab2 SBP mutants confirm critical sulfatide-binding residues

From sulfatide docking studies on wild-type Dab2 SBP, sulfatide docked 8 out of 9 poses clustered near R42 with the sulfate groups being within 5.6 Å of the furthest atoms of the sulfate group in each pose and 1 out of 9 poses residing within 7.4 Å of the cluster group. In addition, HSQC titrations showed that sulfatide markedly perturbed R42 (Supplementary **Fig. S2**), consistent with previous observations [17]. Further molecular docking experiments were performed to confirm the influence of R42 for sulfatide binding. Replacement of R42 to alanine reduced close contacts of Dab2 SBP for sulfatide, as concluded from the analysis of nine independent sulfatide poses on the mutated peptide (**Fig. 3a**, Supplementary **Fig. S3**, and Supplementary **Fig. S8**). Dab2 SBP R42A increased the distance for sulfate head group-A42 interactions to greater than 5.0 Å compared to the wild-type peptide (3.1 Å). To adjust to the loss of R42 in Dab2 SBP R42A, the sulfate head group sought to hydrogen bond with E33 and T35. Interaction fingerprint analysis of Dab2 SBP R42A showed fewer overall interactions (**Fig. 3a**), specifically a loss of aromatic and polar interactions, with sulfatide compared to the wild-type peptide (Supplementary **Table S1**). Docking results also revealed that a mutation of R42 to lysine (R42K) reduced the number of Dab2 SBP contacts with sulfatide (**Fig. 3b** and Supplementary **Fig. S4**) and exhibited less specific docking clusters on the predicted sulfatide-binding site in Dab2 SBP (Supplementary **Fig. S8**), but more closely resembled wild-type Dab2 SBP interactions than R42A. Further analysis indicated that R42K had less aromatic, charged, hydrophobic, and polar interactions but had more hydrogen bond interactions compared to Dab2 SBP (Supplementary **Table S1**). Although Dab2 SBP R42K retains the charged interaction that R42 displayed in Dab2 SBP, the interaction distance between the side chain of K42 and the sulfate head group increased to 3.9 Å. This result indicates that not only the

charge but also the stereochemistry of an arginine residue is required for proper sulfatide docking in Dab2 SBP. Similarly, replacement of Y38 to alanine led Dab2 SBP to have less polar, hydrophobic, and charged interactions with sulfatide while having more backbone and hydrogen bond interactions (Supplementary **Table S1** and **Fig. S5**). Dab2 SBP Y38A increased the interaction distance to 5.0 Å with the sulfate head group (**Fig. 3c** and Supplementary **Fig. S8**), confirming that Y38 plays an important role in sulfatide docking, while not necessarily interacting with the sulfate group itself.

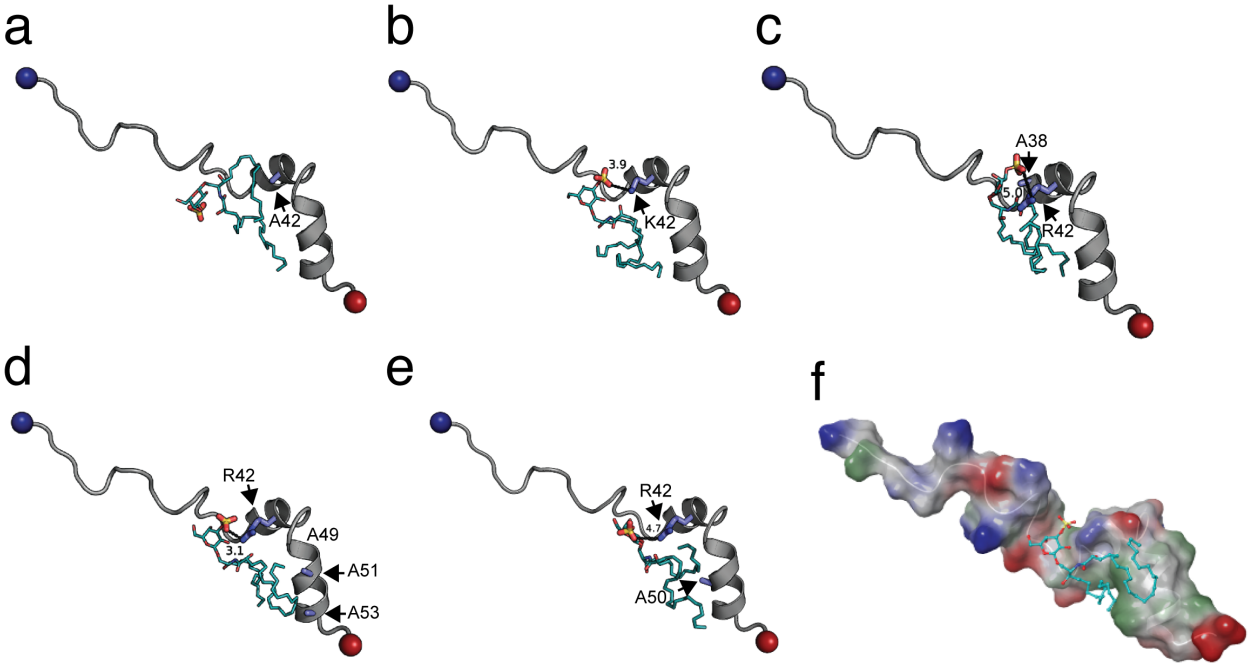

Figure 3. Identification of Dab2 SBP critical residues for sulfatide binding using molecular docking. (**a-e**) Lowest energy pose of sulfatide docked to Dab2 SBP R42A (**a**), Dab2 SBP R42K (**b**), Dab2 SBP Y38A (**c**), Dab2 SBP K49A/K51A/K53A (**d**), and Dab2 SBP Y50A (**e**). In all cases, key residues are colored in blue. Sulfatides (cyan) are shown as sticks and colored by element. (**f**) Surface representation of sulfatide-bound Dab2 SBP K49A/K51A/K53A showing the hydrophobic (green), positively charged (blue), and negatively charged (red) regions. Sulfatide backbone is represented as a stick colored with carbon as cyan, sulfate as yellow and oxygen as red. Surface potential was calculated using Schrodinger Maestro.

Molecular docking of sulfatide in Dab2 SBP predicted lipid acyl chain interactions with residues located in α-helix 2 (**Fig. 3d-e**). Combination mutations at K49, K51, and K53 stabilized the R42 and sulfate head group interaction but influenced acyl tail positioning (**Fig. 3d** and Supplementary **Fig. S6**). This triple mutation in Dab2 SBP showed the same interaction distance as the wild-type

peptide (3.1 Å) with tight sulfate head clustering, as all 9 poses were clustered within 5.5 Å of each other and interacted with R42 compared to 8 out of 9 poses in the wild-type form (Supplementary **Fig. S8**). However, Dab2 SBP K49A/K51A/K53A had less polar, aromatic, and charged interactions while having more backbone and hydrogen bond interactions (Supplementary **Table S1**). The surface rendering of Dab2 SBP K49A/K51A/K53A indicated an exposed hydrophobic area that is less delimited than the wild type Dab2 SBP (**Fig. 3f**), potentially causing a loss of affinity for sulfatide. Thus, these results support the observed environment of Dab2 SBP, generated by residues R42, Y38, K49, K51, and K53, for sulfatide binding. Replacement of Y50 by alanine in the peptide exhibited less total charged and hydrophobic interactions with sulfatide, increasing the sulfate head group distance to R42 to 4.7 Å with a concomitant increment in polar, backbone, and hydrogen bond interactions (**Fig. 3e**, Supplementary **Fig. S7, Fig. S8,** and **Table S1**).

To experimentally assess whether the mutations in Dab2 SBP alter sulfatide binding, recombinant Dab2 SBP, and the mutants identified by docking studies, were fused to glutathione S-transferase (GST) and employed to screen for sulfatide binding using the lipid-protein overlay assay. Although this assay does not mirror the physiological organization of sulfatides in biological membranes, it is still useful for obtaining a first screening for the binding of the Dab2 SBP mutants to the sphingolipid. As expected, Dab2 SBP bound sulfatides and closely reached saturation at 800 pmoles of lipid (**Fig. 4a-b**). Consistent with the molecular docking data, alanine mutations at residues upstream of α-helix 1, such as P32 and Y38 (**Fig. 1a**), reduced the peptide's sulfatide binding, whereas mutations at E33 and R42 markedly diminished it (**Fig. 4**). The poor binding capacity to sulfatides displayed by Dab2 SBP R42A is not due to a disruption of α-helix 1 as it remains as folded as the wild-type peptide, as indicated by their circular dichroism spectra (Supplementary **Fig. S9**). Consistent with the molecular docking studies, replacing R42 by lysine reduced sulfatide binding whereas alanine mutations on residues outside of the predicted binding pocket, such as E37 and D46, did not alter lipid binding (**Fig. 4**). Unexpectedly, alanine mutation of Dab2 SBP at K44, which did not alter the secondary structure of the peptide (Supplementary **Fig. S9**), markedly affected sulfatide binding (**Fig. 4**). Mutagenesis at the second helix, where sulfatide acyl chains may interact, showed that Y50 is not critical for sulfatide binding, but a triple alanine mutation at residues K49, K51, and K53 markedly reduced it (**Fig. 4**) without affecting the secondary structure of the peptide (Supplementary **Fig. S9**). The role of these basic residues in

sulfatide-binding is in agreement with the mutagenesis and liposome-binding studies we previously obtained using Dab2 N-PTB [13].

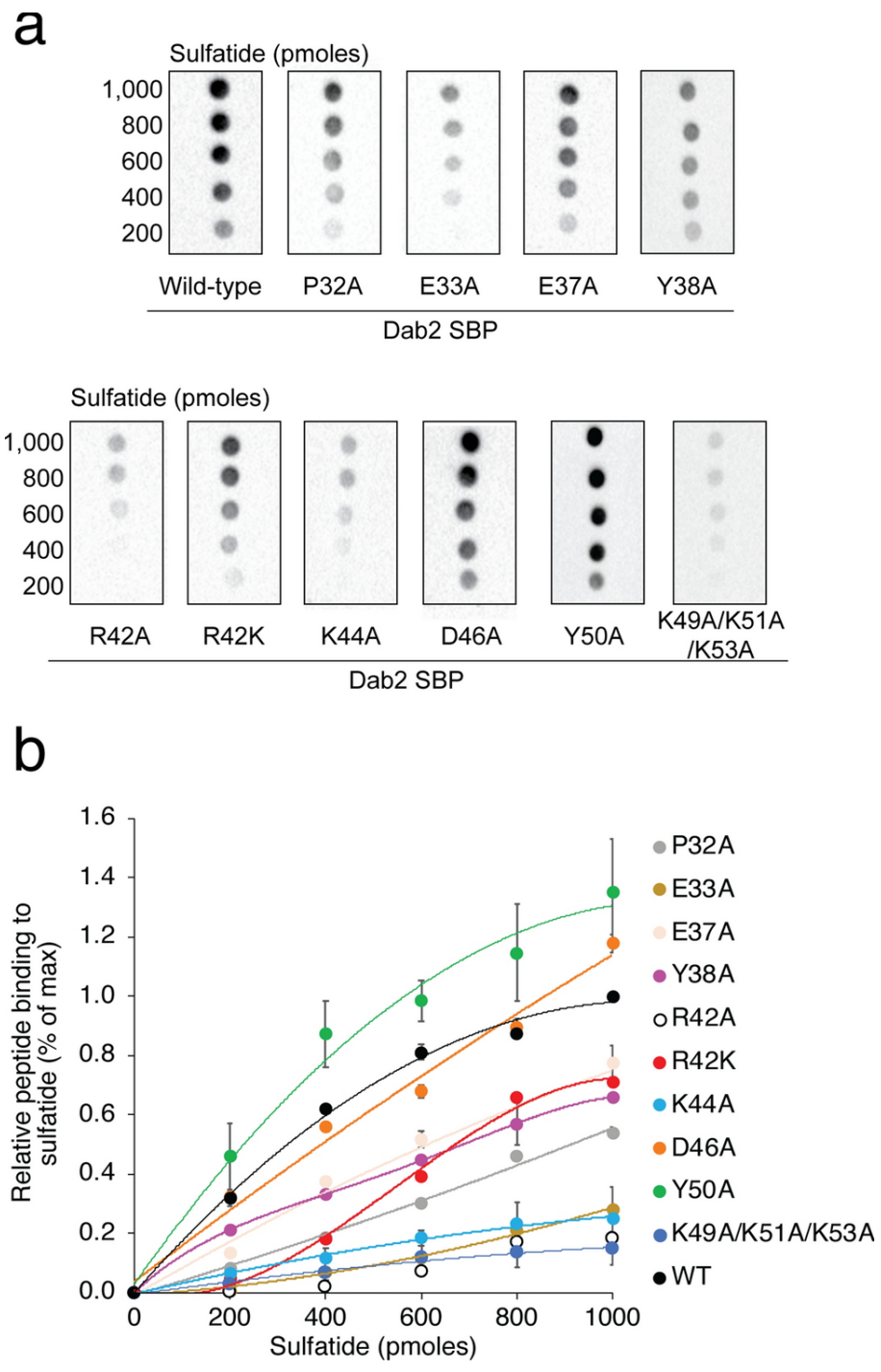

Figure 4. Characterization of sulfatide binding to Dab2 SBP *in vitro*. (**a**) Lipid-protein overlay assay displaying the binding of GST fusion Dab2 SBP and the indicated mutants to sulfatides immobilized on nitrocellulose. (**b**) Quantification of the binding of the GST fusion peptides to sulfatides.

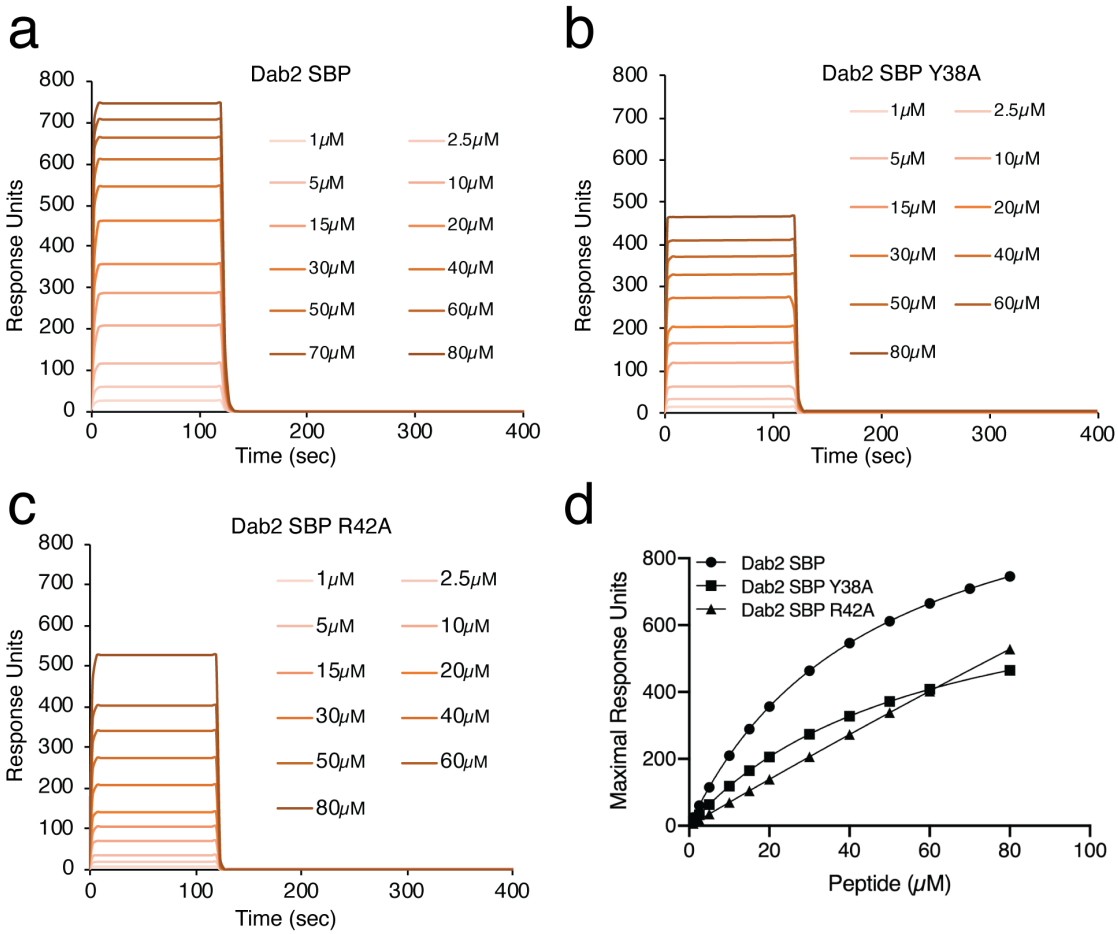

Figure 5. Critical Dab2 SBP residues for binding of mimics of sulfatide-containing lipid bilayers. (**a-c**) SPR traces depicting the binding of Dab2 SBP (**a**), Dab2 SBP Y38A (**b**), and Dab2 SBP R42A (**c**) from 1 to 80 μM, to sulfatide liposomes. (**d**) Plot representing the binding of Dab2 SBP (black circles), Dab2 Y38A (black squares), and Dab2 SBP R42A (black triangles), from 1 to 80 μM, to sulfatide-containing liposomes.

Taking the molecular docking, NMR, and LPOA results together, we next focused on the novel role of the Dab2 SBP residues Y38 and R42 in binding to sulfatides using sulfatide-enriched liposomes of 100 nm in diameter and followed their interactions using surface plasmon resonance (SPR). In agreement with previous observations [17], SPR data showed that Dab2 SBP bound sulfatide liposomes with a K_D of 49.8±5.4 μM and the association displayed saturation of binding (**Fig. 5a** and **d**). Alanine mutation at Y38 exhibited a decrease in sulfatide liposome binding with a K_D of 77.0±6.6 μM (**Fig. 5b** and **d**). Binding of Dab2 SBP R42A to sulfatide liposomes was

weaker, with an estimated K_D higher than 100 μM (**Fig. 5c-d**). Thus, in addition of the role of the α-helix-2 in sulfatide binding, our results show that R42 and Y38, the latter to a lesser extent, are relevant for the association of Dab2 SBP with sulfatide-embedded lipid bilayers.

Dab2 SBP depends on R42 to reduce sulfatide-mediated P-selectin expression

P-selectin is a cell surface pro-aggregatory protein found in platelets and endothelial cells. This protein is stored in α-granules and is quickly released to the platelet surface in response to a wide range of thrombogenic stimuli [18]. P-selectin promotes platelet aggregation in a sulfatide-dependent manner [19]. To establish whether Dab2 SBP can modulate P-selectin pro-aggregatory activity, we evaluated the cell surface expression of P-selectin. Washed platelets were previously activated with ADP, which represents a critical step for sulfatide-mediated platelet activation [20]. Consistent with previous observations [15], incubation of activated platelets with sulfatide-containing liposomes led to an increase in the median fluorescence of the anti-P-selectin antibody bound to the platelet surface (**Fig. 6a**), indicating that sulfatides promote P-selectin accumulation at the platelet surface. Pre-incubation of sulfatide liposomes with Dab2 SBP significantly reduced the presence of P-selectin at the platelet surface (**Fig. 6a**), suggesting that the peptide competes with P-selectin for sulfatide binding. Replacement of R42 with lysine or alanine significantly impaired the Dab2 SBP inhibitory activity (**Fig. 6a**). Representative histograms showing the distribution of the baseline population of platelets is indicated in **Fig. 6b**. As expected, ADP induces a minor right shift, which is indicative of platelet activation (**Fig. 6b**, inset). In contrast to sulfatide-free liposomes, the majority of the platelet population become further activated by the presence of sulfatide liposomes (**Fig. 6b**, inset). In contrast to the presence of either R42A or R42K, the addition of Dab2 SBP led to a shift to the left of the median fluorescence (**Fig. 6b**). Together, our results indicate that Dab2 SBP has the potential to inhibit P-selectin function, with R42 playing a critical role.

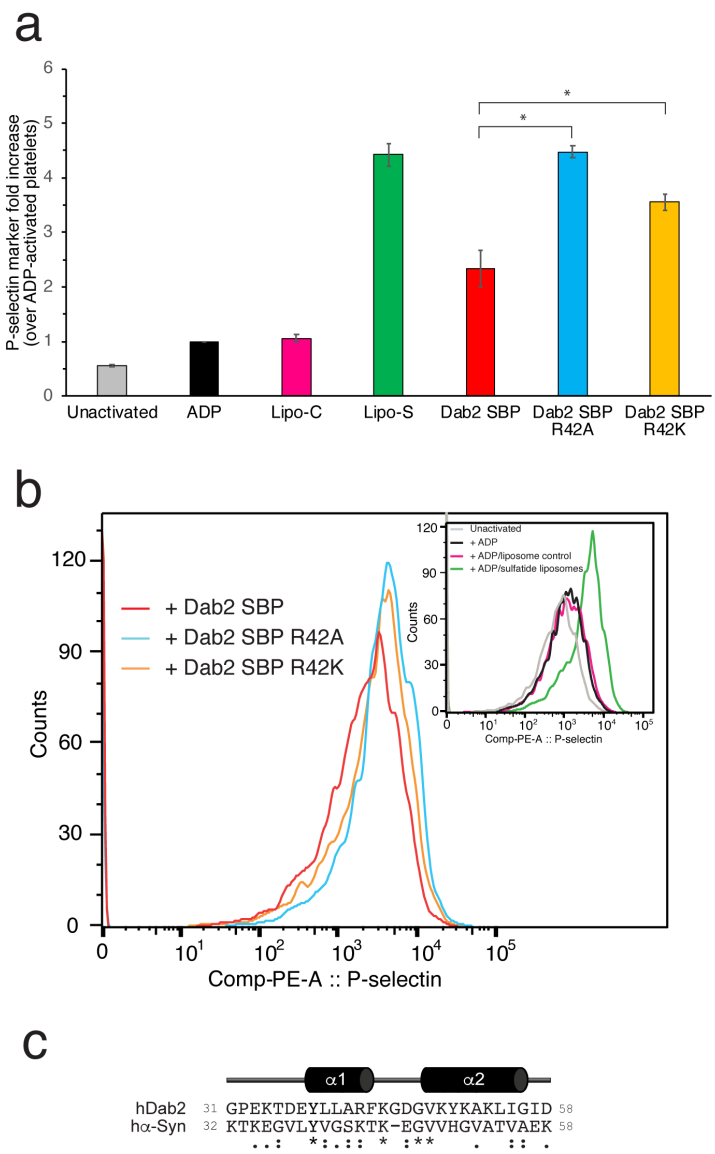

Figure 6. Inhibition of sulfatide-induced platelet P-selectin surface expression in platelets by Dab2 SBP. (**a**) Platelets were stimulated with ADP and further incubated with sulfatide-free (Lipo-C) or sulfatide-containing liposomes (Lipo-S) in the absence or presence of the indicated peptides. Samples were then fixed, incubated with PE-labeled CD62P (anti-P-selectin) antibody, and analyzed by flow cytometry. The graph represents the median fluorescence intensity for each treatment (mean ± standard deviation) of three independent experiments. Data is represented as a fold increase in fluorescence over ADP-treated platelets. Statistical analysis was carried out using a *t*-test. (**b**) Color-coded representative immunofluorescence histogram displaying the presence of platelet surface P-selectin for the treatments indicated in **a**. The gray plot in the inset indicates the presence of P-selectin in the surface of unactivated platelets. (**c**) Comparison of the α-synuclein sphingolipid-binding domain with the sulfatide-binding site of Dab2. Asterisks represent identical residues, whereas residues that share common properties.

Discussion

We previously reported the NMR structure of a region of Dab2 spanning residues 24-58, which we named here Dab2 SBP, binds sulfatide [17]. Furthermore, we showed that the peptide contacts sulfatide-embedded membrane mimics using its twenty C-terminal amino-acids, inhibiting platelet aggregation [17]. In this study, we provide additional structural and functional features of Dab2 SBP. Our molecular docking studies suggest that residues upstream and on the first α-helix of Dab2 SBP interact with the sulfatide head group, whereas the second α-helix provides recognition of the sphingolipid acyl chains. In agreement with the *in silico* data, relaxation measurements showed that sulfatide-dependent motions in Dab2 SBP map in a region comprising residues T35-I56. To establish the structural basis of Dab2 interaction with sulfatides, we designed a series of Dab2 SBP mutants, which were tested for *in silico* docking and *in vitro* sulfatide binding, identifying critical residues for lipid binding. Finally, we demonstrated that the peptide inhibited the platelet surface expression of the pro-aggregatory protein P-selectin in a sulfatide-dependent manner.

Our current results suggest that the Dab2 SBP basic residue, R42, is critical for association to the negatively charged sulfatide. *In silico* results closely matched our experimental results, highlighting the ability of docking to predict key residues for binding sulfatide in Dab2 SBP. Replacement of R42 with lysine reduced sulfatide binding *in vitro* and significantly affected the function of the peptide for targeting P-selectin surface expression in platelets. This result implies that not only the positive charge, but also the stereochemistry of the side chain, is required for sulfatide interactions. In addition, other charged and aromatic Dab2 SBP residues nearby R42 (*i.e.*, E33, Y38, K44) were relevant for lipid interactions. Previous results suggested that the last 20 residues of Dab2 SBP are involved in sulfatide interactions [17]. Mutagenesis analysis of the C-terminal 49-KYKAKL-54 motif (**Fig. 4**) confirmed its role in sulfatide binding. By docking a sulfatide to Dab2 SBP, we found that the C-terminal polybasic motif, located in α-helix 2, is likely required for acyl chain hydrophobic interactions rather than binding to the sphingolipid head group. Lysine residues are considered to exhibit a dual role in lipid contacts by promoting electrostatic interactions with negatively charged lipids and/or by employing their flexible hydrocarbon spacers for hydrophobic interactions with membrane lipids [21]. Indeed, we observe a hydrophobic patch in the wild type Dab2 SBP structure (**Fig. 1d**) that is shaped by K49, K51, and K53. The suggested roles of the α-helices in sulfatide docking are in agreement with the doxyl stearic acid-based

paramagnetic quenching NMR experiments using sulfatide-embedded DPC micelles [17], which demonstrate that the first Dab2 SBP α-helix is less quenched than the second one. Thus, this suggests that the first α-helix is closer to the micellar surface, whereas the second α-helix is oriented towards the micelle core.

Very few protein-sulfatide complexes have been structurally characterized. The interaction of the cluster of differentiation 1a (CD1a) with sulfatide involves hydrogen bonds to its 3' sulfate group with R76 and E154 and the galactose moiety with R76 and S77, whereas the sulfatide fatty acid chains display van der Waals interactions mostly with hydrophobic residues [22]. Interestingly, a basic residue (H38) plays a role in accommodating one of the alkyl chains in the binding pocket of CD1a.

Sphingolipid-binding domains, such as those described in viral, bacterial, and mammalian proteins [23–25], predominantly exhibit a consensus helix-turn-helix fold with an aromatic residue, being solvent-exposed, and either a G or P residue contributing to the turn between the α-helices and several positively charged residues [26]. Intriguingly, a consensus sphingolipid-binding motif has been identified in α-synuclein [27], which shares several features with Dab2 SBP (**Fig. 6c**). Molecular dynamic simulations show that α-synuclein simultaneously interacts with two molecules of the glycosphingolipid monosialodihexosylganglioside (GM3), with Y39 representing the most critical sphingolipid-binding residue [27]. Of note, it is currently unknown whether Dab2 can bind two sulfatide molecules simultaneously. The α-synuclein protein also binds sulfatides, but GM3 represents its preferred ligand [27]. Interestingly, we found that alanine mutation in Dab2 SBP Y38, equivalent to α-synuclein Y39, reduces the affinity for sulfatide binding by ~35%. In the α-synuclein membrane model interaction, it is proposed that Y39 is located at the interface between the polar and nonpolar regions of the sphingolipid, mediating the protein insertion into the membrane [27]. Supportive of this observation, Dab2 Y38 undergoes 30-50% reduction in its resonance intensity in micellar paramagnetic NMR experiments [17]. Accordingly, we observed that Dab2 SBP Y38 exhibited minor dynamic changes when the peptide was in contact with sulfatide-embedded DPC micelles. A basic residue (K34) located upstream of Y39, also displays a major role for α-synuclein interactions with GM3 [27]. However, the equivalent residue in Dab2 SBP, K34, did not exhibit an important role in sulfatide binding as concluded from molecular docking and

NMR assays. In contrast to GM3, sulfatides are negatively charged. Given that α-synuclein has a preference for GM3 over sulfatides, it is possible that α-synuclein K43 may play a similar role to that observed for Dab2 R42 in sulfatide interactions. Considering that R42K mutation in Dab2 SBP reduced the activity of the peptide but did not abolish it, the presence of K43, instead of R43, might also reduce the preference of α-synuclein for sulfatides.

Sulfatides are found in discrete patches on activated spread platelet membranes, reminiscent of lipid rafts. Platelet surface expression of the sulfatide-binding pro-aggregatory protein P-selectin increases the stability of platelet aggregation [20]. Accordingly, Dab2 modulates the extent of platelet aggregation by targeting P-selectin function. The association of Dab2 to sulfatides impairs P-selectin-sulfatide interactions, thereby reducing the formation of platelet aggregates and platelet-leukocyte aggregates [15]. Upon platelet activation, Dab2 is transiently secreted from α-granules to the cell surface [13]. Upon sulfatide binding, Dab2 likely undergoes a conformational change [28], a state in which the protein is more tolerant to thrombin proteolysis [13]. It has been suggested that, once secreted, Dab2 modulates the extent of platelet aggregation by two independent mechanisms [1]. First, Dab2 downregulates the integrin receptor activity by interfering with its interaction with fibrinogen. Second, extracellular Dab2 blocks platelet-platelet P-selectin-mediated sulfatide-dependent interactions. Other sulfatide-binding proteins can be exported out of the cell for extracellular interactions with sulfatides. For example, the mesencephalic astrocyte-derived neurotrophic factor (MANF) is an endoplasmic reticulum protein that is secreted under stress-related stimuli [29]. Binding of secreted MANF to sulfatides, through its α-helical saposin-like domain, provides MANF cellular uptake and alleviates stress responses driven by the endoplasmic reticulum [30].

In conclusion, our results indicate how sulfatides interact with Dab2 SBP and identify the critical binding residues. Our data is in line with what was earlier defined as the minimal α-helical-turn-α-helical unit for sphingolipid binding. Furthermore, in the case of Dab2, we suggest that R42 mediates the recognition of the negatively charged sulfatide headgroup, and the α-helical lysine residues at the C-terminus provide an adequate hydrophobic environment through their flexible hydrocarbon spacers.

Methods

Chemicals

The list of chemicals and their suppliers are: brain sulfatides, 1,2-dipalmitoyl-sn-glycero-3-phosphocholine (DPPC), 1,2-dipalmitoyl-sn-glycero-3-phosphoethanolamine (DPPE) (Avanti-Lipids), N-dodecylphosphocholine (DPC) (Anatrace), cholesterol (Sigma), and isopropyl β-D-thiogalactopyranoside (Research Products International). All other chemicals were of analytical grade.

Expression and purification of Dab2 SBP

A cDNA, representing residues 24-58 in hDab2, was cloned into a pGEX6P1 vector (GE Healthcare). A GST fusion and untagged Dab2 SBP were expressed and purified as described [31]. Site-directed mutagenesis of Dab2 SBP was carried out using the QuikChange (Stratagene) protocol.

Creation and validation of Dab2 SBP models

Energy minimized Dab2 SBP and its mutant structures were created with Schrödinger-Maestro v2018-3 [32], using the NMR-derived, Dab2 SBP DPC-micelle embedded structure [PDB ID: 2LSW [17]] as a template. To align with the experimental peptide sequence in this work, residues 19-23 (GPLGS) were built onto the N-terminus of PDB ID: 2LSW using Schrödinger-Maestro's 3D-Builder. Following the addition of residues 19-23 to the template structure, energy minimization was performed using the OPLS3e forcefield [33] and default settings in Schrödinger-Maestro v2018-3. After energy minimization, the Dab2 SBP structure was exported into PDB format and model quality was assessed using several validation methods. Ramachandran plots generated using the Rampage webserver [34] assessed model quality with respect to favorable and allowed φ and ψ angles of residues, and SWISS-MODEL [35,36] calculated a QMEAN plot to quantify model quality with respect to solvation and torsion angle. ProSA [37,38] compared the model to experimentally derived structures similar in composition. Five mutant peptides were individually created using the energy minimized Dab2 SBP structure as the starting template. Each mutation (Y38A, R42A, R42K, K49A/K51A/K53A, and Y50A) was built using Schrödinger-Maestro [32] by altering the residue(s) of interest using the built-in mutagenesis tool. Following residue alteration, energy minimization was performed as stated above. Structures were exported as PDB files and model quality was assessed using the same procedure as Dab2 SBP, with varying validation quality as influenced by the point mutations.

Molecular docking of Dab2 SBP variants to sulfatide

The structure of sulfatide was obtained from the ZINC database (ZINC96006133) and converted from the mol2 to the PDB format using UCSF Chimera [38]. Sulfatide and Dab2 SBP and point mutation structures were prepared in AutoDockTools v1.5.6 [39] and a sulfatide was docked to each Dab2 SBP energy minimized structure using AutoDock Vina v1.1.2 [40]. The same grid box and center was used for each docking experiment and covered the entire Dab2 SBP structure. The center coordinates for the grid box (X, Y, Z) were (-1.722, 0.667, -2.2194). The grid box dimensions (X, Y, Z) were (30Å, 46Å, 42Å), using a 1 Å grid space. Nine poses were created from each docking run, with the lowest energy pose used for further analysis on residue interaction and fingerprint analysis. Molecular visualization of docked poses was performed in PyMOL [41]. Sulfatide pose volume occupancy was visualized using UCSF Chimera. Schrödinger-Maestro's Interaction Fingerprints analysis tool was used with default parameters on each lowest energy docked pose to determine potential peptide-sulfatide interactions. The output matrix was converted manually to a table format and organized by interaction type.

NMR spectroscopy

^{15}N-labeled Dab2 SBP (1 mM) was prepared in 90% H_2O, 10% ^2H_2O, 10 mM d_4-citrate (pH 5.0), 40 mM KCl, 1 mM NaN_3, and 200 mM d_{38}-DPC in the absence or presence of 8 mM sulfatide. A Bruker Avance III 800 spectrometer with cryoprobe and standard Bruker two dimensional ^{1}H–^{15}N HSQC-type pulse sequences were used to obtain ^{15}N longitudinal (R_1) and transverse (R_2) relaxation rates, and ^{1}H–^{15}N NOEs of Dab2 SBP in the absence and presence of sulfatide at 25°C. The pulse sequences were hsqcnoef3gpsi (Het-NOE), hsqct1etf3gpsi3d (R_1), and hsqct2etf3gpsi3d (R_2) [all from Bruker]. Relaxation delays for the R_1 experiments were 5, 50, 150, 250, 400, 550, 750, 1200, and 2000 ms. Relaxation delays for the R_2 experiments were 17, 34, 51, 68, 119, 153, 203, and 254 ms. The recycle delay for R_1 and R_2 experiments was 2 s. ^{1}H–^{15}N NOEs were measured by comparing intensities of ^{1}H–^{15}N correlation spectra with either 5 s of ^{1}H saturation or a 5 s delay preceding ^{1}H–^{15}N correlation.

Lipid-protein overlay assay

Sulfatide strips were prepared by spotting 1 µl of the indicated amount of sulfatides, dissolved in chloroform/methanol/water (1:2:0.8), onto a Hybond-C extra membrane (GE Healthcare). Membrane strips were blocked with 3% fatty acid-free BSA (Sigma) in 20 mM Tris-HCl (pH 8.0), 150 mM NaCl, and 0.1% Tween-20 for 1 h at room temperature. Then, membrane strips were

incubated with the indicated GST fusion peptide in the same buffer overnight at 4°C. Following four washes with the same buffer, bound fusion peptides were detected with rabbit anti-GST antibody (Proteintech) and donkey anti-rabbit-horseradish peroxidase antibody (GE Healthcare). Binding of fusion peptides to sulfatides was probed using the Supersignal West Pico chemiluminescent reagent (Pierce).

Surface plasmon resonance

Binding of Dab2 SBP peptides to sulfatide liposomes were monitored by surface plasmon resonance (SPR) at room temperature using a BIAcore X-100 instrument (GE Healthcare). One-hundred nanometer size-calibrated liposomes were generated as previously described. Briefly, lipids including DPPC:DPPE:cholesterol (1:1:1; control), or DPPC:DPPE:cholesterol:sulfatide (1:1:1:4), were solubilized in chloroform/methanol/water mixtures. The resulting mixture was dried under N_2 followed by vacuum to remove solvent traces. The lipid mixture was then resuspended at 0.8 mg/ml in 20 mM Tris-HCl (pH 6.8) and 100 mM NaCl to reach a final concentration of 0.5 mM sulfatide, sonicated, and extruded for 100-nm liposome size at 68°C. L1 sensorchips were first equilibrated with 20 mM Tris-HCl (pH 7.4) and 100 mM NaCl as a running buffer. Then, L1 sensorchips were pretreated with 40 mM octyl β-D-glucopyranoside. At a 30 μl/min flow rate, control liposomes were immobilized onto one of the L1 sensorchip channels whereas a second channel was loaded with sulfatide-containing liposomes. Typical liposome loading was ~4,000 response units/sensorchip channel. The apparent K_D values were estimated using BIAevaluation software, version 2.0 (GE Healthcare).

Blood collection and platelet purification

Blood samples were obtained from healthy volunteers by venipuncture, according to Virginia Tech Institutional Review Board guidelines. Blood samples were collected into vacutainer ACD solution A blood tubes (Becton, Dickinson and Co) and centrifuged for 20 min at 200xg to separate a platelet-rich plasma (PRP) fraction from erythrocytes. Then, the PRP fraction was further centrifuged for 5 min at 1,100x*g*. The resultant platelet-containing pellet was resuspended in 10 mM HEPES (pH 7.4), 134 mM NaCl, 12 mM $NaHCO_3$, 2.9 mM KCl, 0.34 mM Na_2HPO_4, and 1 mM $MgCl_2$ (Tyrode's buffer) containing 0.5 μM prostaglandin (PGI_2). Platelets were then washed in PGI_2-free Tyrode's buffer, containing 5 mM dextrose and 0.3% BSA, and counted in a haemocytometer.

Flow cytometry

Washed platelets (1.5 x 10^5 platelets/μl) were maintained in Tyrode's buffer (unactivated) or treated with 30 μM ADP (activated). Both unactivated and activated platelets were incubated for 6 min at room temperature with either control liposomes (Lipo-C, 50 μg/ml) or sulfatide-containing liposomes (Lipo-S, 50 μg/ml) in the absence and presence of 50 μM of one of the following peptides: Dab2 SBP, Dab2 SBP R42A, or Dab2 SBP R42K. Platelets were fixed with 1% formalin in phosphate buffered saline and incubated with phycoerythrin-labelled anti-CD62P (P-selectin; Biolegend) antibody following manufacturer's instructions. Antibody-bound platelets were quantified using a FacsAria flow cytometer.

Acknowledgements

We thank Dr. Janet Webster for critical reading of the manuscript. This project was supported by the Virginia Academy of Science, the Institute for Critical Technology and Applied Science (ICTAS) at Virginia Tech, the 4-VA Collaborative Research Program (to D.G.S.C.), and the National Science Foundation (MCB-1517298) (to C.V.F). W.S. was supported by an ICTAS pre-doctoral fellowship.

References

1. Finkielstein, C. V. & Capelluto, D. G. S. Disabled-2: A modular scaffold protein with multifaceted functions in signaling. *BioEssays* **38**, S45–S55 (2016).
2. Howell, B. W., Gertler, F. B. & Cooper, J. A. Mouse disabled (mDab1): A Src binding protein implicated in neuronal development. *EMBO J.* **16**, 121–132 (1997).
3. Xu Wannian Yang, Suzanne Jackowski, and Charles O. Rock, X.-X. Cloning of a Novel Phosphoprotein Regulated by Colony-stimulating Factor 1 Shares a Domain with the Drosophiladisabled Gene Product. *J. Biol. Chem.* **270**, 14184–14191 (1995).
4. Sheng, Z. *et al.* Restoration of positioning control following Disabled-2 expression in ovarian and breast tumor cells. *Oncogene* **19**, 4847–4854 (2000).
5. Zhou, J., Scholes, J. & Hsieh, J. T. Characterization of a novel negative regulator (DOC-2/DAB2) of c-Src in normal prostatic epithelium and cancer. *J. Biol. Chem.* **278**, 6936–6941 (2003).
6. Karam, J. A. *et al.* Decreased DOC-2/DAB2 expression in urothelial carcinoma of the bladder. *Clin. Cancer Res.* **13**, 4400–4406 (2007).
7. Kleeff, J. *et al.* Down-regulation of DOC-2 in colorectal cancer points to its role as a tumor

suppressor in this malignancy. *Dis. Colon Rectum* **45**, 1242–1248 (2002).

8. Fulop, V. *et al.* DOC-2/hDab2, a candidate tumor suppressor gene involved in the development of gestational trophoblastic diseases. *Oncogene* **17**, 419–424 (1998).
9. Huang, C. L. *et al.* Disabled-2 is a negative regulator of integrin αIIbβ3-mediated fibrinogen adhesion and cell signaling. *J. Biol. Chem.* **279**, 42279–42289 (2004).
10. Rivera, J., Lozano, M. L., Navarro-Núñez, L. & Vicente García, V. Platelet receptors and signaling in the dynamics of thrombus formation. *Haematologica* **94**, 700–711 (2009).
11. Stefanini, L. & Bergmeier, W. Negative regulators of platelet activation and adhesion. *J. Thromb. Haemost.* **16**, 220–230 (2018).
12. Huang, C.-L. *et al.* Disabled-2 is a novel alphaIIb-integrin-binding protein that negatively regulates platelet-fibrinogen interactions and platelet aggregation. *J. Cell Sci.* **119**, 4420–4430 (2006).
13. Drahos, K. E., Welsh, J. D., Finkielstein, C. V & Capelluto, D. G. S. Sulfatides partition disabled-2 in response to platelet activation. *PLoS One* **4**, (2009).
14. Xiao, S., Finkielstein, C. V. & Capelluto, D. G. S. The Enigmatic Role of Sulfatides: New Insights into Cellular Functions and Mechanisms of Protein Recognition. in *Advances in experimental medicine and biology* **991**, 27–40 (Adv Exp Med Biol, 2013).
15. Welsh, J. D. *et al.* Disabled-2 modulates homotypic and heterotypic platelet interactions by binding to sulfatides. *Br. J. Haematol.* **154**, 122–133 (2011).
16. Merten, M. & Thiagarajan, P. P-selectin expression on platelets determines size and stability of platelet aggregates. *Circulation* **102**, 1931–1936 (2000).
17. Xiao, S. *et al.* Structure, Sulfatide Binding Properties, and Inhibition of Platelet Aggregation by a Disabled-2 Protein-derived Peptide. *J. Biol. Chem.* **287**, 37691–37702 (2012).
18. Furie, B., Furie, B. C. & Flaumenhaft, R. A journey with platelet P-selectin: the molecular basis of granule secretion, signalling and cell adhesion. *Thromb. Haemost.* **86**, 214—221 (2001).
19. Merten, M. *et al.* Sulfatides activate platelets through P-selectin and enhance platelet and platelet-leukocyte aggregation. *Arterioscler. Thromb. Vasc. Biol.* **25**, 258–263 (2005).
20. Hoernke, M., Schwieger, C., Kerth, A. & Blume, A. Binding of cationic pentapeptides with modified side chain lengths to negatively charged lipid membranes: Complex interplay of electrostatic and hydrophobic interactions. *Biochim. Biophys. Acta - Biomembr.* **1818**,

1663–1672 (2012).

21. Zajonc, D. M., Elsliger, M. A., Teyton, L. & Wilson, I. A. Crystal structure of CD1a in complex with a sulfatide self antigen at a resolution of 2.15 Å. *Nat. Immunol.* **4**, 808–815 (2003).
22. Delézay, O., Hammache, D., Fantini, J. & Yahi, N. Spc3, a V3 loop-derived synthetic peptide inhibitor of HIV-1 infection, binds to cell surface glycosphingolipids. *Biochemistry* **35**, 15663–15671 (1996).
23. Fantini, J., Garmy, N. & Yahi, N. Prediction of glycolipid-binding domains from the amino acid sequence of lipid raft-associated proteins: Application to HpaA, a protein involved in the adhesion of Helicobacter pylori to gastrointestinal cells. *Biochemistry* **45**, 10957–10962 (2006).
24. Taïeb, N. *et al.* The first extracellular domain of the tumour stem cell marker CD133 contains an antigenic ganglioside-binding motif. *Cancer Lett.* **278**, 164–173 (2009).
25. Fantini, J. How sphingolipids bind and shape proteins: Molecular basis of lipid-protein interactions in lipid shells, rafts and related biomembrane domains. *Cell. Mol. Life Sci.* **60**, 1027–1032 (2003).
26. Fantini, J. & Yahi, N. Molecular basis for the glycosphingolipid-binding specificity of α-synuclein: Key role of tyrosine 39 in membrane insertion. *J. Mol. Biol.* **408**, 654–659 (2011).
27. Alajlouni, R., Drahos, K. E., Finkielstein, C. V. & Capelluto, D. G. S. Lipid-mediated membrane binding properties of Disabled-2. *Biochim. Biophys. Acta - Biomembr.* **1808**, 2734–2744 (2011).
28. Liu, H., Tang, X. & Gong, L. Mesencephalic astrocyte-derived neurotrophic factor and cerebral dopamine neurotrophic factor: New endoplasmic reticulum stress response proteins. *Eur. J. Pharmacol.* **750**, 118–122 (2015).
29. Bai, M. *et al.* Conserved roles of C. elegans and human MANFs in sulfatide binding and cytoprotection. *Nat. Commun.* **9**, 1–11 (2018).
30. Xiao, S., Zhao, X., Finkielstein, C. V. & Capelluto, D. G. S. A rapid procedure to isolate isotopically labeled peptides for NMR studies: Application to the Disabled-2 sulfatide-binding motif. *J. Pept. Sci.* **20**, 216–222 (2014).
31. Schrödinger Release 2018-3: Maestro, S., LLC, New York, NY(2018).
32. Harder, E. *et al.* OPLS3: A Force Field Providing Broad Coverage of Drug-like Small

Molecules and Proteins. *J. Chem. Theory Comput.* **12**, 281–296 (2016).

33. Lovell, S. C. *et al.* Structure validation by Cα geometry: φ,ψ and Cβ deviation. *Proteins Struct. Funct. Genet.* **50**, 437–450 (2003).
34. Waterhouse, A. *et al.* SWISS-MODEL: Homology modelling of protein structures and complexes. *Nucleic Acids Res.* **46**, W296–W303 (2018).
35. Benkert, P., Biasini, M. & Schwede, T. Toward the estimation of the absolute quality of individual protein structure models. *Bioinformatics* **27**, 343–350 (2011).
36. Wiederstein, M. & Sippl, M. J. ProSA-web: Interactive web service for the recognition of errors in three-dimensional structures of proteins. *Nucleic Acids Res.* **35**, 407–410 (2007).
37. Sippl, M. J. Recognition of errors in three-dimensional structures of proteins. *Proteins Struct. Funct. Bioinforma.* **17**, 355–362 (1993).
38. Pettersen, E. F. *et al.* UCSF Chimera - A visualization system for exploratory research and analysis. *J. Comput. Chem.* **25**, 1605–1612 (2004).
39. Morris, G. M. *et al.* AutoDock4 and AutoDockTools4: Automated Dockingwith Selective Receptor Flexibility. *J. Comput. Chem.* **30**, 2785–2791 (2009).
40. Trott, O. & Olson, A. NIH Public Access. *J. Comput. Chem.* **31**, 455–461 (2010).
41. Schrödinger, L. The PyMol Molecular Graphics System, Versión 1.8 (2015).

Supplementary information

Material and Methods

Circular dichroism

Far-UV (190-250 nm) circular dichroism (CD) spectra were collected using a Jasco PFD-425 S temperature control unit-equipped J-815 spectropolarimeter at 10 μM Dab2 SBP constructs in 10 mM citrate (pH 5), 40 mM KF and in the presence of 10 mM DPC. Five CD spectral accumulations were collected at a 1-nm bandwidth with a response time of 1 s and at a scan speed of 20 nm/min at 23°C. Buffer spectra were also recorded under the same experimental conditions and subtracted from the peptide spectra.

Tables and figures

Table S1. Residue-sulfatide interactions of the lowest energy pose of Dab2 SBP. Residue interactions were determined using Schrödinger-Maestro.

Dab2 SBP

Interaction Type	Backbone	Polar	Hydrophobic	Hydrogen Bond Acceptor	Hydrogen Bond Donor	Aromatic	Charged Residue
Residues	K30 P32 E33 K34 T35	E33 T35 D36 R42 K49 K51	Y38 L39 F43 Y50 L54 I55			Y38 F43 Y50	E33 D36 R42 K49 K51

Dab2 SBP R42A

Interaction Type	Backbone	Polar	Hydrophobic	Hydrogen Bond Acceptor	Hydrogen Bond Donor	Aromatic Residue	Charged Residue
Residue	K30 P32 E33 K34 T35	K29 E33 T35 K49 K53	P32 Y38 L39 A42 Y50 L54			Y38 Y50	K29 E33 K49 K53

Dab2 SBP Y38A

Interaction Type	Backbone	Polar	Hydrophobic	Hydrogen Bond Acceptor	Hydrogen Bond Donor	Aromatic Residue	Charged Residue
Residue	K30 G31 P32 K34 T35 A38	T35 R42 D46 K49	P32 A38 L39 Y50 L54	T35	R42	Y50	R42 D46 K49

	L39 L54						

Dab2 SBP K49A/K51A/K53A

Interaction Type	Backbone	Polar	Hydrophobic	Hydrogen Bond Acceptor	Hydrogen Bond Donor	Aromatic Residue	Charged Residue
Residue	K30 P32 E33 K34 T35 A49 Y50	K29 E33 T35 R42 D46	Y38 L39 A49 Y50 A53 L54	Y50		Y38 Y50	K29 E33 R42 D46

DAB2 SBP Y50A

Interaction Type	Backbone	Polar	Hydrophobic	Hydrogen Bond Acceptor	Hydrogen Bond Donor	Aromatic Residue	Charged Residue
Residue	K30 P32 E33 D46 G47 A50 K51 K53	K29 K30 E33 T35 R42 K51 K53	Y38 L39 A50 L54	K30		Y38	K29 K30 E33 R42 K51 K53

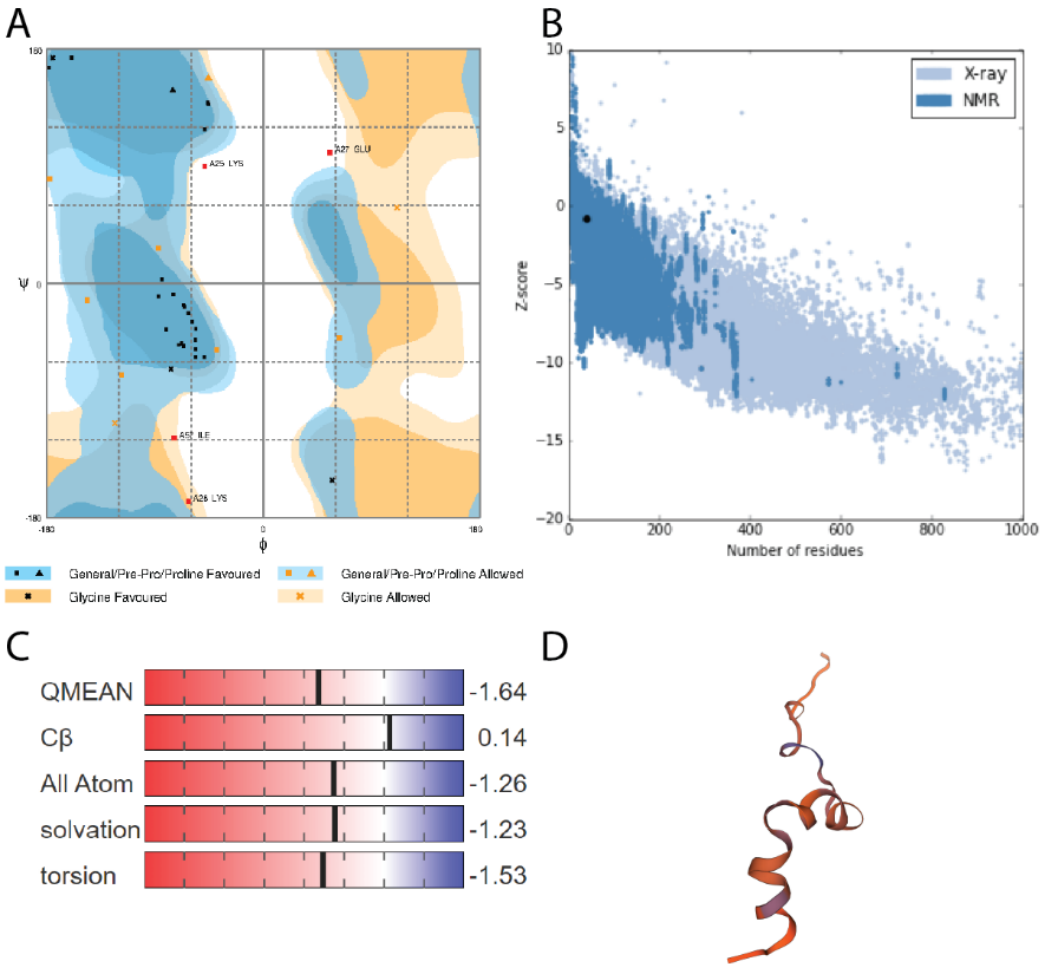

Fig. S1. Model validation of Dab2 SBP after energy minimization. (**A**) Ramachandran plot of (φ, ψ) angles for all residues represented as favorable and allowed (black and yellow squares, triangles, and Xs, 89.5%) and outlier (red squares, triangles, and Xs, 10.5%). (**B**) ProSA Z-Score represented as a black dot on the blue plot (-0.84) comparing structure to similar sequence length proteins resolved by NMR or x-ray crystallography. (**C**) Summary of QMEAN scores assessing structure quality based on solvation and torsion angle. (**D**) 3D-Model of QMEAN structure assessment scores mapped onto model.

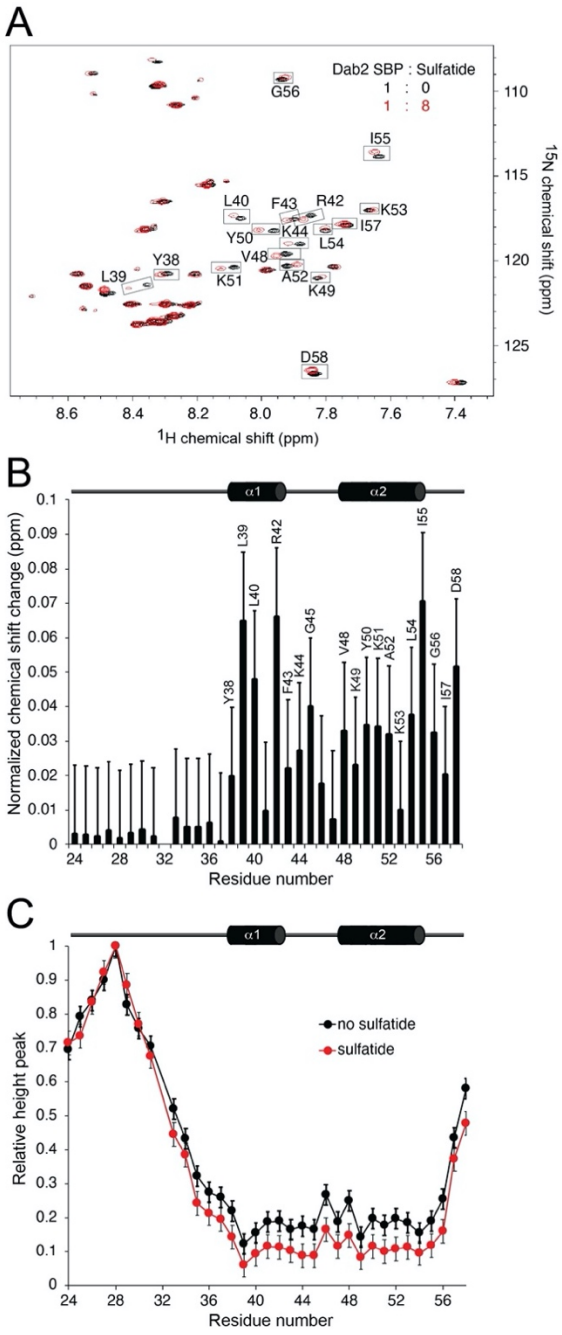

Fig. S2. The interaction of Dab2 SBP with sulfatides followed by two-dimensional NMR spectroscopy. (**A**) HSQC spectrum of Dab2 SBP in the absence (black) and presence of DPC-embedded sulfatide. Most perturbed resonances are labeled and boxed. (**B**) Histogram representing the normalized NMR resonance changes of DPC-embedded Dab2 SBP induced by DPC-embedded sulfatides. Dab2 SBP amino acids that display markedly chemical shift changes are labeled. (**C**) Histogram representing the intensity of the NMR resonances of DPC-embedded Dab2 SBP relative to residue K28 in the absence (black) and presence (red) of DPC-embedded sulfatides. Secondary structure of Dab2 SBP is represented at the top of each panel.

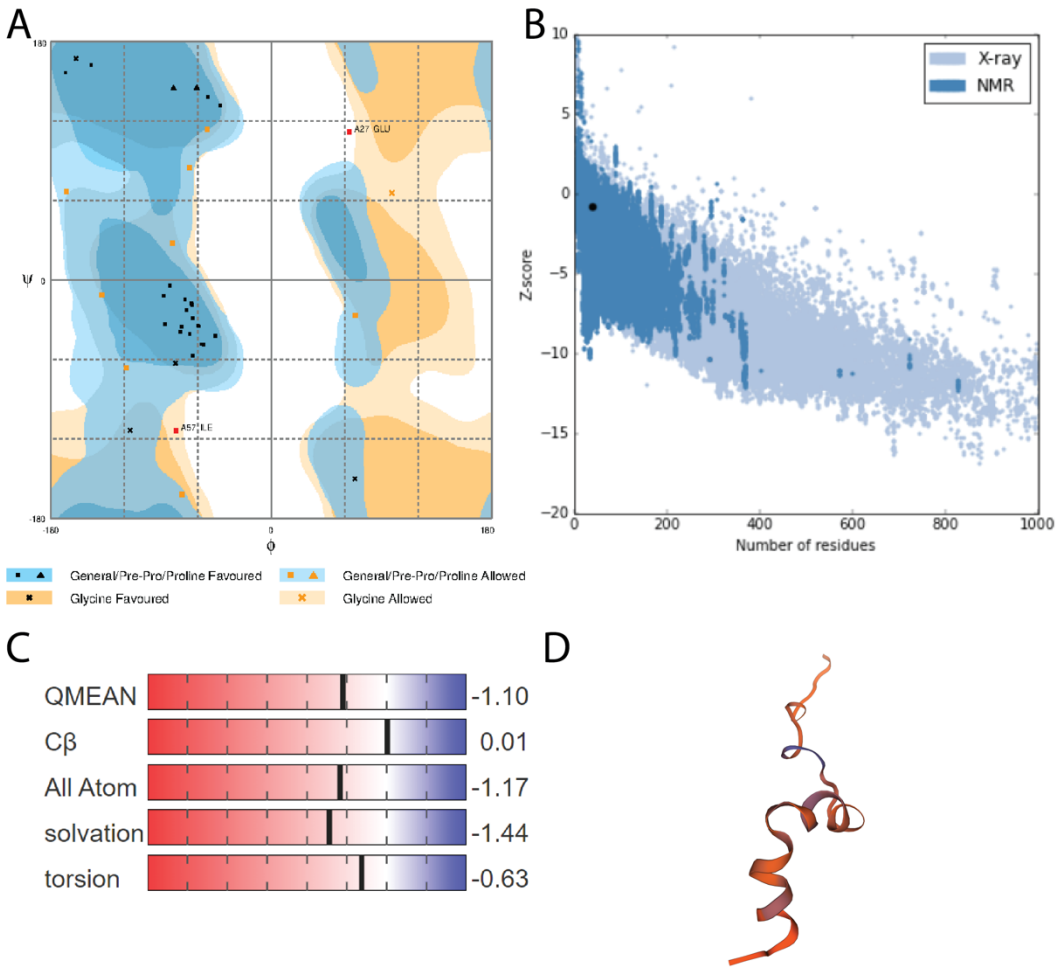

Fig. S3. Model validation of Dab2 SBP R42A after energy minimization. (**A**) Ramachandran plot of (φ, ψ) angles for all residues represented as favorable and allowed (black and yellow squares, triangles, and Xs, 94.7%) and outlier (red squares, triangles, and Xs, 5.3%). (**B**) ProSA Z-Score represented as a black dot on the blue plot (-0.8) comparing structure to similar sequence length proteins resolved by NMR or x-ray crystallography. (**C**) Summary of QMEAN scores assessing structure quality based on solvation and torsion angle. (**D**) 3D-Model of QMEAN structure assessment scores mapped onto model.

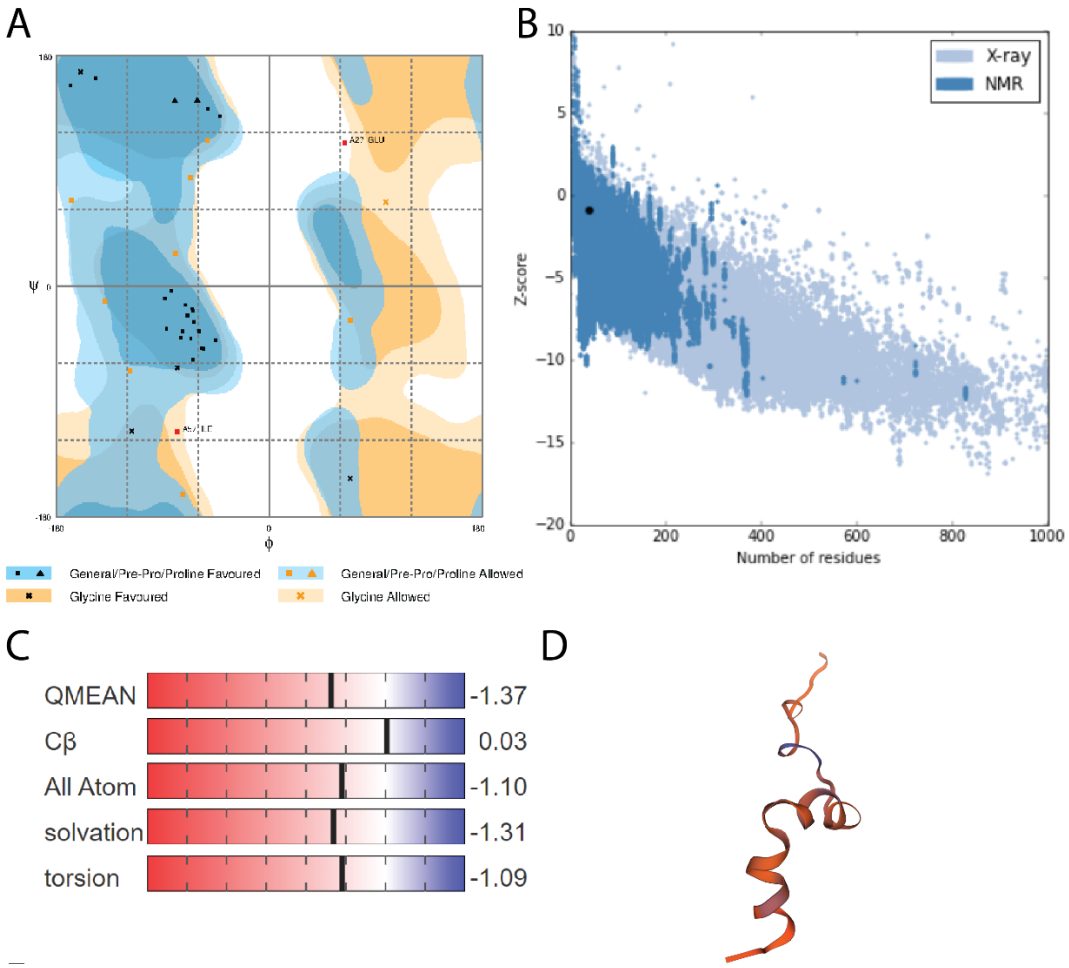

Fig. S4. Model validation of Dab2 SBP R42K structure after energy minimization. (**A)** Ramachandran plot of (φ, ψ) angles for all residues represented as favorable and allowed (black and yellow squares, triangles, and Xs, 94.7%) and outlier (red squares, triangles, and Xs, 5.3%). (**B**) ProSA Z-Score represented as a black dot on the blue plot (-0.9) comparing structure to similar sequence length proteins resolved by NMR or x-ray crystallography. (**C**) Summary of QMEAN scores assessing structure quality based on solvation and torsion angle. (**D**) 3D-Model of QMEAN structure assessment scores mapped onto model.

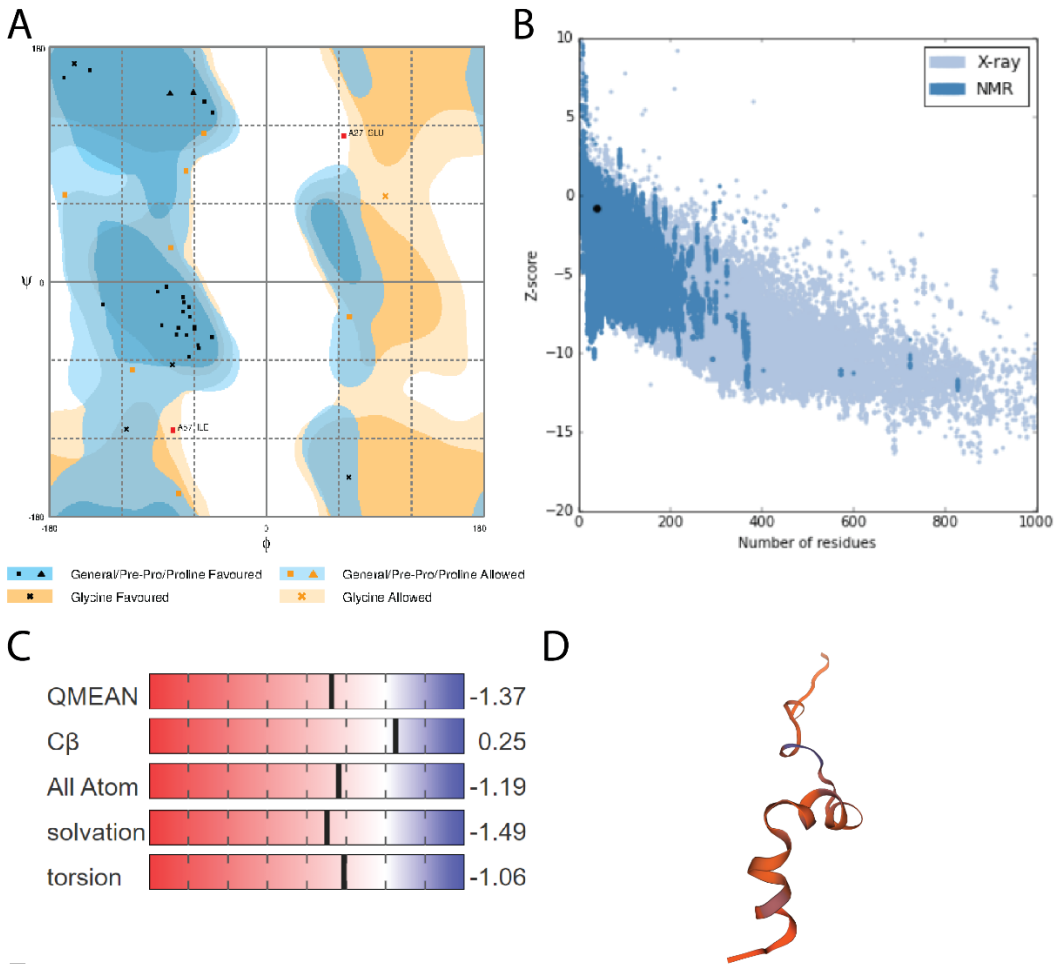

Fig. S5. Model validation of Dab2 SBP Y38A after energy minimization. (**A**) Ramachandran plot of (φ, ψ) angles for all residues represented as favorable and allowed (black and yellow squares, triangles, and Xs, 94.7%) and outlier (red squares, triangles, and Xs, 5.3%). (**B**) ProSA Z-Score represented as a black dot on the blue plot (-0.78) comparing structure to similar sequence length proteins resolved by NMR or x-ray crystallography. (**C**) Summary of QMEAN scores assessing structure quality based on solvation and torsion angle. (**D**) 3D-Model of QMEAN structure assessment scores mapped onto model.

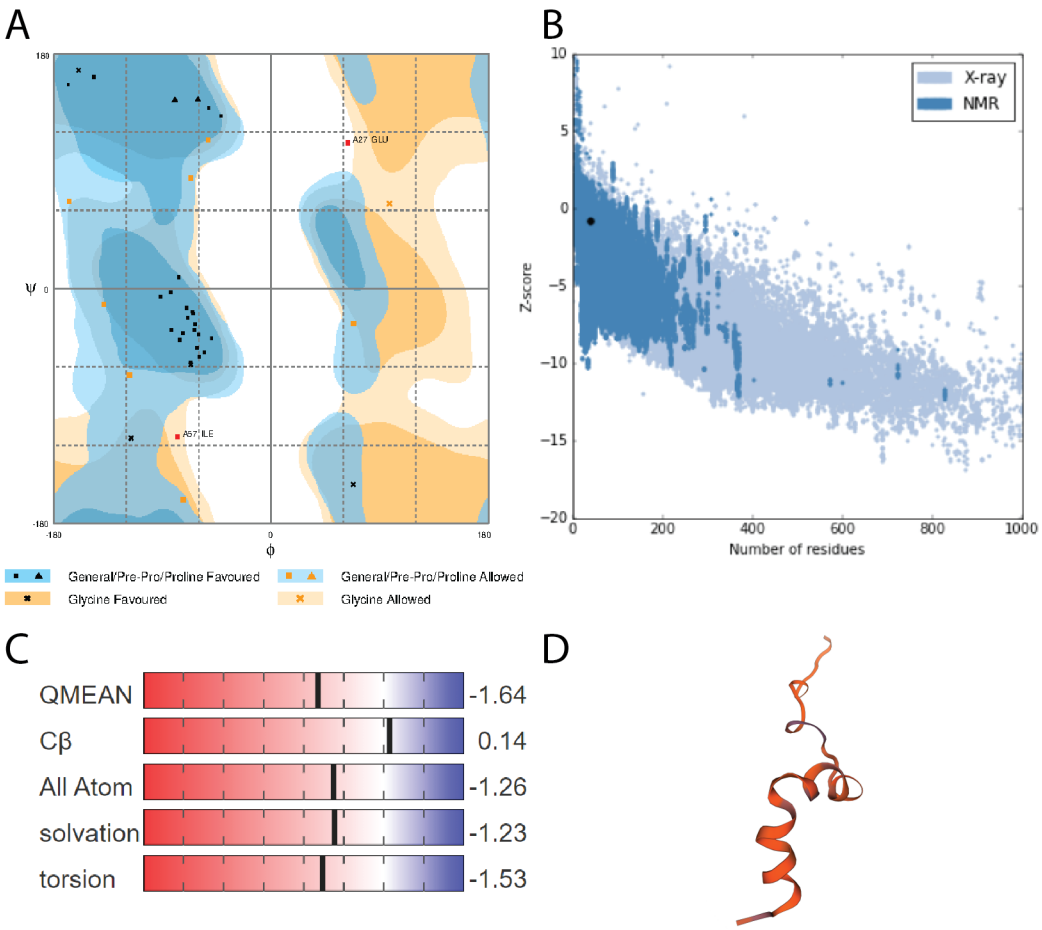

Fig. S6. Model validation of Dab2 SBP K49A/K51A/K53A Dab2 after energy minimization. (**A**) Ramachandran plot of (φ, ψ) angles for all residues represented as favorable and allowed (black and yellow squares, triangles, and Xs, 94.7%) and outlier (red squares, triangles, and Xs, 5.3%). (**B**) ProSA Z-Score represented as a black dot on the blue plot (-0.77) comparing structure to similar sequence length proteins resolved by NMR or x-ray crystallography. (**C**) Summary of QMEAN scores assessing structure quality based on solvation and torsion angle. (**D**) 3D-Model of QMEAN structure assessment scores mapped onto model.

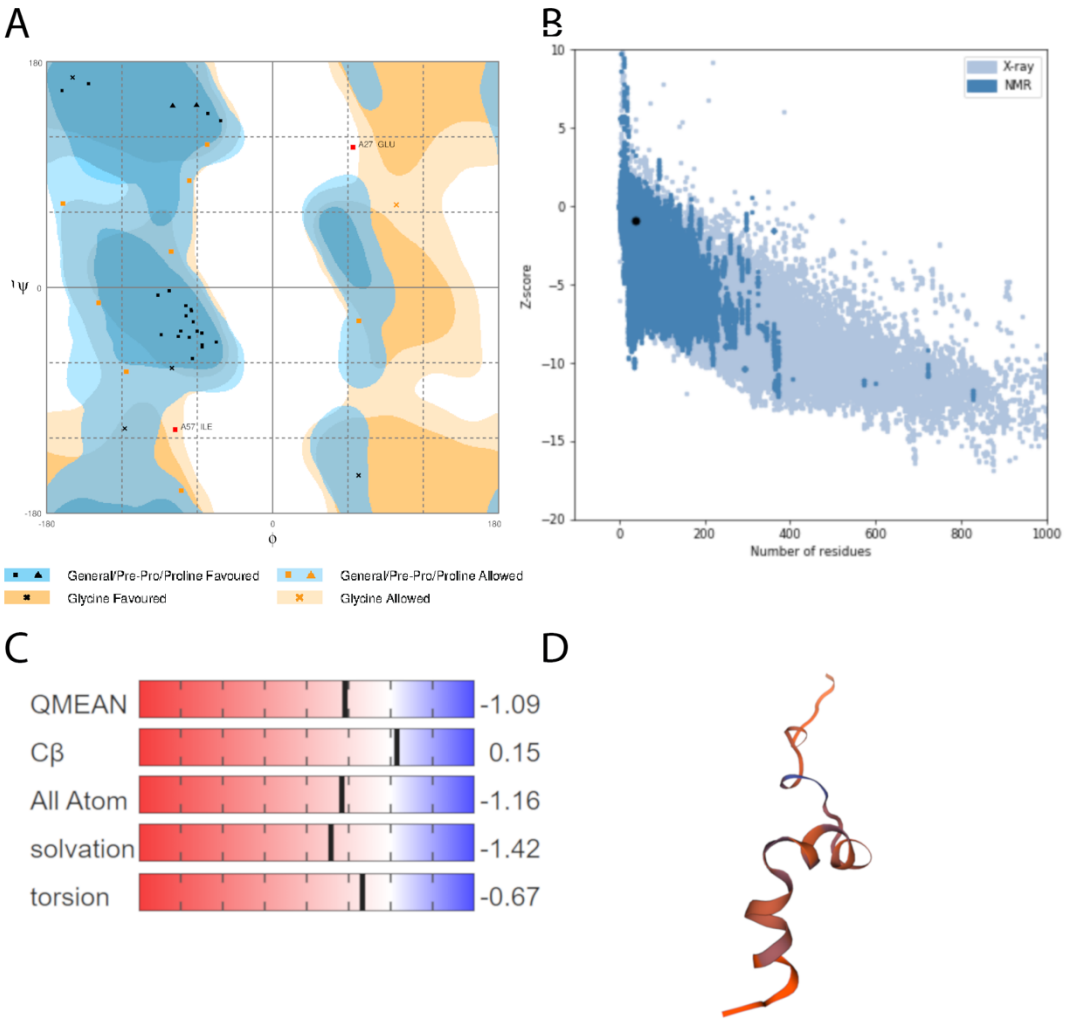

Fig. S7. Model validation of Dab2 SBP Y50A structure after energy minimization. **(A)** Ramachandran plot of (φ, ψ) angles for all residues represented as favorable and allowed (black and yellow squares, triangles, and Xs, 94.7%) and outlier (red squares, triangles, and Xs, 5.3%). **(B)** ProSA Z-Score represented as a black dot on the blue plot (-0.89) comparing structure to similar sequence length proteins resolved by NMR or x-ray crystallography. **(C)** Summary of QMEAN scores assessing structure quality based on solvation and torsion angle. **(D)** 3D-Model of QMEAN structure assessment scores mapped onto model.

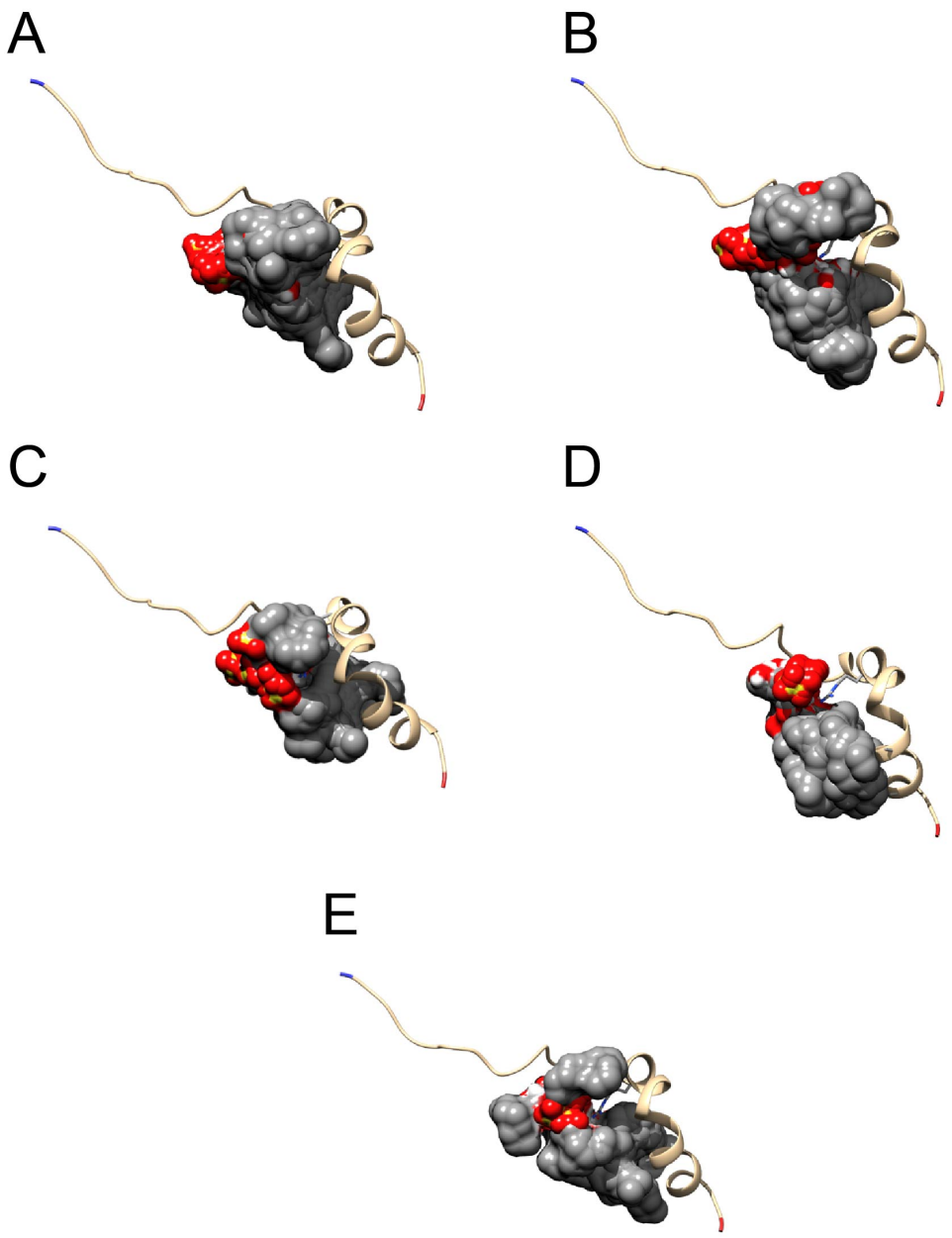

Fig. S8. Surface representation of all sulfatide poses docked to Dab2 SBP mutants. (**A**) Dab2 SBP R42A; (**B**) Dab2 SBP R42K; (**C**) Dab2 SBP Y38A; (**D**) Dab2 SBP K49A/K51A/K53A; (**E**) Dab2 SBP Y50A. Dab2 SBP mutant structures are rendered as cartoon colored tan with the N-terminus colored blue and C-terminus colored red. R42, when visible, is shown as stick colored gray and by atom type. Sulfatide head groups are colored red with their sulfo groups yellow, whereas the acyl chains are colored gray. The nine poses, produced by AutoDock Vina, are shown as surface colored gray and by atom type.

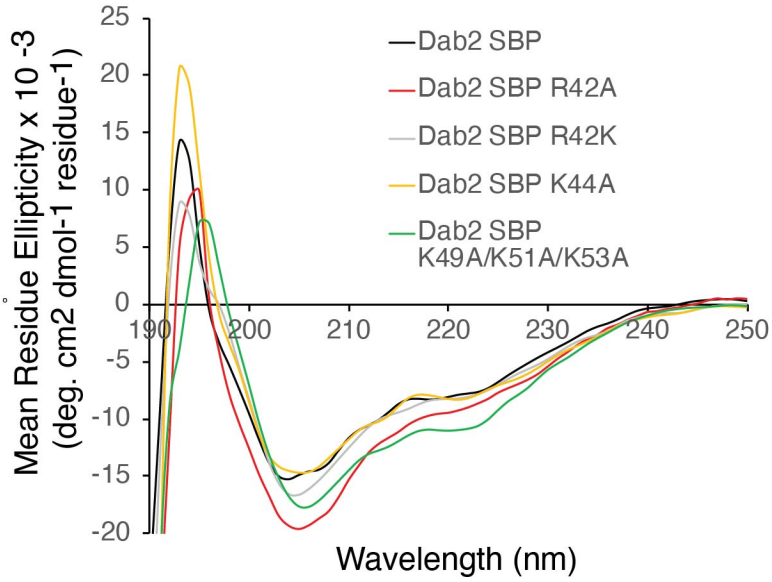

Fig. S9. Far-UV CD spectra of DPC-embedded Dab2 SBP (black), Dab2 SBP R42A (red), Dab2 SBP R42K (gray), Dab2 SBP K44A (orange), and Dab2 SBP K49A/K51A/K53A (green).

Chapter 3 Conclusions

The results of this work elucidated the fundamental mechanisms of Dab2 SBP binding to sulfatide with both structural and functional perspectives, which can be used for the design of Dab2 SBP-derived peptides that may interfere with platelet-platelet and platelet-cancer cell interaction by competing with P-selectin for sulfatide association. The resulted findings are listed below:

(1) Autodock Vina has been used to refine the residues involved in the interaction between sulfatide and Dab2 SBP and its derived peptides. Molecular docking showed that Arg42 is one of the most critical residues of Dab2 SBP for sulfatide interaction through the recognition of the negatively charged sulfatide headgroup. Two mutants, Dab2 SBP R42A and Dab2 SBP R42K, were designed further to evaluate the binding mechanism and the same docking procedures as Dab2 SBP were performed. Accordingly, both the positive charge and the stereochemistry of the side chain are found to be necessary for sulfatide interactions. Also, several charged and aromatic residues around R42 (i.e., E33, Y38, K44) facilitated lipid interactions. Moreover, we found that the C-terminal polybasic motif, located in the second α-helix, is likely required for acyl chain hydrophobic interactions rather than binding to the sulfatide head group.

(2) In order to better understand the binding mechanism between sulfatide and Dab2 SBP, the backbone dynamics of Dab2 SBP was determined by solution NMR spectroscopy. The results showed that the addition of sulfatide embedded in DPC micelle to Dab2 SBP has little or no effect on ^{1}H and ^{15}N chemical shifts of the N-terminal residues (24-31), but alters the shifts of most residues at the C-terminus (35-56), which agrees with our previous studies. The heights of NHSQC peaks for residues 35-56 are considerably lower than peak heights for residues 24-31 for both Dab2 SBP in DPC with and without sulfatide. Residues 35-56 may not be observable with solution NMR when Dab2 SBP is attached to liposomes. The NMR relaxation data indicates that sulfatide has little or no effect on motions of residues 24-31 but shifts the spectral density of residues 35-56 to lower frequency. This could be due to sulfatide binding to residues 35-56, consistent with the data from molecular docking and HSQC titrations of the peptide with the lipid, or a sulfatide-induced increase in DPC micelle size or both.

(3) To experimentally evaluate whether the mutations in Dab2 SBP affect sulfatide binding, several recombinant Dab2 SBP mutants were designed based on the molecular docking studies and employed to lipid-protein overlay assay (LPOA). Compared to the wild-type Dab2 SBP,

mutants with alanine mutations at residues upstream of α-helix 1, such as P32A and Y38A, reduced the peptide's sulfatide binding, whereas mutants E33A and R42A dramatically diminished it. In addition, Dab2 SBP R42K reduced the sulfatide binding. However, mutants with mutations outside of the predicted binding pocket, such as E37A and D46A, did not alter lipid binding. Mutations at the second helix showed that Tyr50 is not critical for sulfatide binding, but a triple alanine mutation at residues Lys49, Lys51, and Lys53 markedly reduced it without affecting the secondary structure of the peptide. These observations are consistent with molecular docking studies. It is worthy to notice that all the mutations did not affect the peptides' overall secondary structures, as evidenced by circular dichroism studies.

(4) Based on the above results, we next focused on the role of the Dab2 SBP residues Y38 and R42 in sulfatides binding using surface plasmon resonance (SPR). The data showed that Dab2 SBP binds to sulfatide-loaded liposomes with a K_D of 49.8±5.4 μM and the association displayed saturation of binding. In contrast, alanine mutation at Y38 showed a decreased sulfatide liposome binding with a K_D of 77.0±6.6 μM. Dab2 R42A bound sulfatide-loaded liposomes showed a weaker binding affinity, estimated higher than 100 μM. Collectively, these results suggest that Arg42 and Tyr38, the latter to a lesser extent, are relevant for the association of Dab2 SBP with sulfatide-embedded lipid bilayers.

(5) Furthermore, flow cytometry was conducted to assess whether Dab2 SBP can modulate P-selectin pro-aggregatory activity as P-selectin promotes platelet aggregation in a sulfatide-dependent manner. Pre-incubation of sulfatide liposomes with Dab2 SBP significantly reduced the presence of P-selectin at the platelet surface, indicating that the peptide competes with P-selectin for sulfatide binding. However, Dab2 SBM R42A abolished its ability to inhibit sulfatide-induced P-selection expression at the platelet surface, while Dab2 SBM R42K induced a less significant P-selectin expression than Dab2 SBP. Therefore, our results suggest that Dab2 SBP has the potential to inhibit P-selectin function, with Arg42 playing a critical role.

Collectively, this work provides the dissection of the structural basis for sulfatide recognition by Dab2 with various biophysical approaches. Also, the biological activities of Dab2 in inhibiting platelet activation through P-selectin competition for sulfatide binding are determined by flow cytometry. Studies on the role of platelet activation in cancer cell metastasis indicate that platelet can be a potent target for cancer therapy. It is known that Dab2 transiently presents at the surface of activated platelets. Therefore, with the development of newer and more efficient drug-delivery

systems, our findings raise the possibility of using a Dab2 SBP-derived peptide with altered sulfatide recognition features in platelets to target the site of CTCs without causing severely impaired platelet activation and bleeding risk. Accordingly, the resulting peptide might compete with P-selectin on the platelet and cancer cell surface to limit platelet aggregation and platelet adhesion to cancer cells, respectively, thus working as an antiplatelet drug with anticancer properties.